HHS Public Access

Author manuscript

J Comp Neurol. Author manuscript; available in PMC 2021 November 01.

Published in final edited form as:

J Comp Neurol. 2020 November 01; 528(16): 2708–2728. doi:10.1002/cne.24927.

Central afferents to the nucleus of the solitary tract in rats and mice

Silvia Gasparini, **Jacob M. Howland**, **Andrew J. Thatcher**, **Joel C. Geerling**

Department of Neurology, Iowa Neuroscience Institute, University of Iowa

Abstract

The nucleus of the solitary tract (NTS) regulates life-sustaining functions ranging from appetite and digestion to heart rate and breathing. It is also the brain's primary sensory nucleus for visceral sensations relevant to symptoms in medical and psychiatric disorders. To better understand which neurons may exert top-down control over the NTS, here we provide a brain-wide map of all neurons that project axons directly to the caudal, viscerosensory NTS, focusing on a medial subregion with aldosterone-sensitive HSD2 neurons. Injecting an axonal tracer (cholera toxin b) into the NTS produces a similar pattern of retrograde labeling in rats and mice. The paraventricular hypothalamic nucleus (PVH), lateral hypothalamic area, and central nucleus of the amygdala (CeA) contain the densest concentrations of NTS-projecting neurons. PVH afferents are glutamatergic (express *Slc17a6*/Vglut2) and are distinct from neuroendocrine PVH neurons. CeA afferents are GABAergic (express *Slc32a1*/Vgat) and are distributed largely in the medial CeA subdivision. Other retrogradely labeled neurons are located in a variety of brain regions, including the cerebral cortex (insular and infralimbic areas), bed nucleus of the stria terminalis, periaqueductal gray, Barrington's nucleus, Kölliker-Fuse nucleus, hindbrain reticular formation, and rostral NTS. Similar patterns of retrograde labeling result from tracer injections into different NTS subdivisions, with dual retrograde tracing revealing that many afferent neurons project axon collaterals to both the lateral and medial NTS subdivisions. This information provides a roadmap for studying descending axonal projections that may influence visceromotor systems and visceral "mind-body" symptoms.

Keywords

Solitary nucleus; nucleus of the solitary tract; nucleus tractus solitarius; nucleus tractus solitarii; paraventricular; hypothalamus; retrograde tracing; insular cortex; medial prefrontal cortex; infralimbic

*Correspondence to: Joel C. Geerling, MD, PhD, joel-geerling@uiowa.edu, PBDB-1320, 169 Newton Rd., Iowa City, IA 52246.

Role of Authors

SG and JCG planned experiments; SG performed all injections; JMH and SG plotted CTb retrogradely labeled neurons; SG and JCG prepared and edited figures; SG drafted the manuscript; SG and JCG edited the manuscript. JCG supervised the project. All authors reviewed and discussed the results and contributed to the final manuscript.

Introduction

The nucleus of the solitary tract (NTS) regulates life-sustaining functions including appetite, digestion, breathing, and blood pressure (Barnett et al., 2017; Jarvie & Palmiter, 2017; Moreira et al., 2009; Resch et al., 2017; Roman et al., 2016; Williams et al., 2018). The NTS often is referred to as the vagal viscerosensory nucleus because it receives synaptic input directly from the vagus nerve (cranial nerve X), which innervates a variety of visceral structures including the gut, lungs, and heart (Altschuler et al., 1991; Corbett et al., 2005; Kalia & Mesulam, 1980; Norgren & Smith, 1988). The NTS also receives gustatory and other information via cranial nerves VII and IX (Contreras et al., 1982; Hamilton & Norgren, 1984; May & Hill, 2006).

The NTS has been divided into three levels (rostral, intermediate, and caudal) and contains two subdivisions (lateral and medial), plus a commissural region trailing beneath the area postrema (Ganchrow et al., 2014; Herbert et al., 1990). These subregions contain several subnuclei, which integrate and transmit different information (Ganchrow et al., 2014; Herbert et al., 1990). Gustatory afferents innervate taste-relay neurons in the rostral NTS (Ganchrow et al., 2014; May & Hill, 2006), while vagal input from the esophagus selectively targets the central NTS subnucleus, whose neurons control esophageal peristalsis (Cunningham & Sawchenko, 1990). Pulmonary vagal afferents innervate the lateral NTS to modulate pulmonary reflexes (Bonham & McCrimmon, 1990; Chang et al., 2015; Kalia & Mesulam, 1980), while gastrointestinal vagal afferents deliver postingestive signals to the medial NTS (Norgren & Smith, 1988; Williams et al., 2016). Baroreceptor afferents target a separate, dorsolateral subregion of the medial NTS subdivision (Chan et al., 2000; Ciriello, 1983; Guyenet, 2006), and chemoreceptor afferents innervate the caudal commissural NTS (Finley & Katz, 1992).

In this study, we focus on afferents from within the brain, rather than peripheral inputs, particularly afferents to the large, medial subdivision at intermediate and caudal levels of the NTS. This region contains a subpopulation of neurons that are distinguished by their expression of the enzyme 11-β-hydroxysteroid dehydrogenase 2 (HSD2). HSD2 neurons increase their activity specifically in association with sodium appetite and drive mice to consume salt (Geerling, Engeland, et al., 2006; Geerling, Kawata, et al., 2006; Jarvie & Palmiter, 2017; Resch et al., 2017). Both the natriorexigenic hormone aldosterone and angiotensin II stimulate HSD2 neurons (Resch et al., 2017), but the sources of synaptic input to these neurons remain obscure. They receive abundant appositions from glutamatergic and GABAergic presynaptic boutons, yet little or no input from the vagus nerve (Resch et al., 2017; Shin et al., 2008). We have identified candidate inputs from other neurons in the NTS and area postrema (Sequeira et al., 2006) and from the hypothalamus and amygdala (Geerling & Loewy, 2006a; Geerling et al., 2010), but we lack comprehensive and detailed information about all the possible sources of input to HSD2 neurons and the surrounding NTS.

NTS neurons are known to integrate descending information from the forebrain with vagal input from the viscera (Banks & Harris, 1987). Some neurons receive the bulk of their synaptic input from inside the brain, with little or no direct input from the periphery (Bailey

et al., 2006; Kawai & Senba, 1996; Resch et al., 2017; Shin et al., 2009). By modulating visceral sensory input, forebrain afferents may be important for “mind-body” symptoms in a variety of medical and psychiatric diseases, where our understanding of the neural basis for visceral sensations and visceromotor changes remains incomplete. Our goal in this study is to identify and begin characterizing the brain-wide set of neurons that are positioned to alter visceral sensations by projecting axons directly to the NTS.

In rats, previous tracing studies identified brain regions that project axons to the NTS. These include: insular and medial prefrontal cortex, bed nucleus of the stria terminalis, central nucleus of the amygdala, hypothalamus, Kölliker-Fuse, ventrolateral medulla, and raphe nuclei (Geerling & Loewy, 2006a; Geerling et al., 2010; Goto & Swanson, 2004; Hardy, 2001; Krukoff et al., 1993; Menetrey & Basbaum, 1987; Ross et al., 1981; Schaffar et al., 1988; Sofroniew, 1983; Terenzi & Ingram, 1995; Terreberry & Neafsey, 1983; Thor & Helke, 1988; Torrealba & Muller, 1996; van der Kooy et al., 1984). In mice, however, information is restricted to gustatory regions of the rostral NTS (Ganchrow et al., 2014). There is no comprehensive information about afferents to the caudal, viscerosensory region in mice. Also, there are no head-to-head comparisons of NTS afferents between rats and mice, and we have little information in any species regarding the fast neurotransmitter identity of neurons that project axons to the NTS.

Here, we use retrograde axonal tracing to map the brain-wide distribution of neurons that project axons to the medial subdivision of the NTS in rats. We then map this distribution in mice and identify the fast neurotransmitter identity of afferent neurons in the hypothalamus and amygdala. Our results identify the overall set of neurons with potential synaptic connectivity to viscerosensory neurons in the NTS.

Materials and Methods

Animals.

The experiments were performed in Sprague Dawley rats and in male C57bl/6J (20-30 g) mice. Rat neuroanatomical tracing was described in two previous reports (Geerling & Loewy, 2006a; Geerling et al., 2010). Mice were housed in a University of Iowa mouse barrier facility on a 12:12-h light-dark cycle with monitored temperature (21–23°C) and humidity (30 – 40%). Water and standard rodent chow were available *ad libitum*. All experiments were approved and conducted in accordance with the guidelines of the Institutional Animal Care and Use Committee at the University of Iowa.

Stereotaxic injections.

We iontophoresed CTb into the medial NTS in rats as described previously (Geerling & Loewy, 2006a; Geerling et al., 2010). Briefly, rats (n = 11; Harlan Sprague-Dawley, male and female; body weight range 250-400 g at the time of surgery) were anesthetized with sodium pentobarbital (50 mg/kg, i.p.), and we iontophoresed CTb (0.1% low-salt CTb in distilled water; #104, List Biological) through a glass micropipette with the tip positioned 0.5 mm rostral to the calamus scriptorius, 0.2 mm right, and 0.45 mm deep. All rats

recovered fully within an hour after injection, were monitored daily, and were perfused transcardially one week later.

To map afferents to NTS, mice (n = 19; C57B6/J, male and female; body weights 19-31 g at the time of surgery) were anesthetized with isoflurane (0.5-1.5%, titrated to respiratory depth and rate) and placed into a stereotaxic apparatus (Kopf 1900) with the head angled down. After a midline incision, we retracted skin and muscle to expose the atlanto-occipital membrane atop the fourth ventricle, then used a 28-gauge needle or scalpel to incise it, providing access to the dorsal medulla. We injected 20 to 30 nl of cholera toxin β-subunit (0.1% solution of salt-free CTb made in distilled water, List, lot #10331A1) with a fine-tipped micropipette (20-30 μm inner diameter) into the NTS using controlled puffs of compressed air, typically 0.5-1 per second, with a target rate of 5-10 nL per minute. We targeted injections to the medial NTS subdivision, where the HSD2 neurons are located, using calamus scriptorius as a stereotaxic reference point. In mice, the pipette was positioned 0.15 mm rostral to calamus scriptorius, 0.15 mm lateral (right side) and 0.45 mm deep. The injection lasted 3-5 minutes, after which the pipette was left in place for an additional 5 minutes. After removing the pipette slowly from the site, the skin was closed with Vetbond (3M). Meloxicam (1 mg/kg s.c.) was provided for postoperative analgesia, along with lactated Ringer's solution (0.5 mL s.c.). All mice awoke from isoflurane anesthesia within 1-2 minutes. Following recovery from anesthesia, mice were monitored daily, injected with meloxicam again 24 hours after surgery, and perfused 1-5 days after CTb injection.

To label PVH neuroendocrine neurons that project to the median eminence and pituitary, in three of these mice we intraperitoneally (i.p.) injected 300 μl Fluorogold (0.2% w/v in 0.9% sterile saline; Fluorochrome) on the same day as CTb microinjection into the NTS. Intraperitoneal or intravenous injection of this and other blood-brain-barrier (BBB)-restricted tracers is a standard technique for retrogradely labeling neuroendocrine and motor neurons in the brain, which extend axons to the median eminence or other targets outside the BBB (Biag et al., 2012; Merchenthaler, 1991).

To examine the possibility of separate descending afferents to the lateral versus medial NTS subdivisions, in three additional mice we microinjected Fluorogold (2%, 30 nl) into the lateral NTS subdivision (0.8 mm deep, 0.15 mm rostral, and 0.8 mm lateral to calamus scriptorium) after injecting CTb into the medial NTS subdivision as above.

Perfusion and tissue sectioning.

Mice were anesthetized with ketamine-xylazine (150 mg/kg and 15 mg/kg i.p.) and perfused 24-72 hours after CTB injections. We perfused them through the ascending aorta with phosphate buffered saline (Sigma P7059 10x, diluted to 1x using deionized water; pH 7.40 at 23 °C), followed by 10% formalin-PBS (Fisher SF100). Brains were post-fixed for 24 hours in 10% formalin-PBS followed by 24 hours in 30% sucrose-PBS. After placing a shallow, thin cut, with a fine razor blade to mark the right-side cerebral cortex and ventral brainstem, each brain was cut in the transverse plane using a freezing microtome (American Optical 860; PhysiTemp BFS-40MPA). Sections were 40 μm-thick and every 3rd section was collected into a separate (1-in-3) series. Tissue sections were stored in cryoprotectant

solution at −20°C. We selected NTS sections from one series to immunolabel HSD2 and CTB. After checking the site of injection, we labeled all the sections of another series for CTB using DAB. Finally, we used sections from a third series to perform RNAscope *in situ* hybridization for glutamatergic or GABAergic neuron markers.

Immunostaining.

To check the sites of the injections in mice, we labeled a 1:3 series of NTS sections for CTb with a goat polyclonal antiserum (1:10,000; List Biological, 703, lot # 7032A9) and for HSD2 with a rabbit polyclonal antiserum (1:700; Santa Cruz, sc.20176, lot # B0609). Both antibodies were diluted in a solution containing 0.25% Triton X-100 (BP151-500, Fisher) and 2% donkey serum (NDS, 017-000-121, Jackson ImmunoResearch) in 0.05% sodium azide (14314, Alfa Aesar) as a preservative (PBT-NDS-azide). On the next morning, tissue was washed 3x in PBS (1-2 min each) and incubated for 2 hours in secondary antibodies: Alexa Fluor 488 Donkey anti-goat (1:500; Jackson ImmunoResearch, West Grove, PA) and Cy3-conjugated anti-rabbit (1:1000; Jackson, ImmunoResearch West Grove, PA). We washed the tissue 3-5 times in PBS between each step. Slides were coverslipped using Vectashield with DAPI (Vector Labs).

Next, in n=15 cases with confirmed CTb injections into the NTS, we performed ABC-DAB staining (immunohistochemistry) in a full-brain 1-in-3 series to map retrogradely labeled neurons. Tissue sections were washed 3x with PBS and transferred to 0.3% H_2O_2 for 30 minutes to suppress endogenous peroxidase activity. Tissue was 3x rinsed with PBS and incubated overnight with the same primary antibody against CTb. On the next morning, we washed the slices 3x with PBS (1-2 min per wash) and incubated the tissue with a biotinylated donkey anti-goat secondary antibody solution (1:500; Jackson ImmunoResearch, West Grove, PA) for 2 hours, followed by 3x PBS washes then avidin-biotin complex for 1h (ABC, Vectastain ABC kit PK-6100; Vector). After that, sections were washed 3x in PBS and transferred to a diaminobenzidine (DAB) solution for 10 min. Our stock DAB solution was prepared by adding 100 tablets (#D-4418; Sigma) into 200 mL of distilled-deionized water (ddH_2O), then vacuum-filtering it. We then used 1 mL of this DAB stock solution per 6.5 mL PBS. After 10 minutes in DAB, we added hydrogen peroxide (0.8 μL of 30% H_2O_2 per 1 mL PBS-DAB) and swirled sections for 1-3 min until observing brown (DAB) color change. Then, we did the final two rinses in PBS and mounted the slices on gelatinized glass slides, air-dried, and Cytoseal (Thermo Scientific, Waltham, MA) was used to coverslip.

To analyze Fluorogold and CTb labeling in n=3 cases after dual injections into the NTS, we incubated sections with the same primary CTb antibody described above along with guinea pig anti-Fluorogold (1:1,000; Protos-Biotech, product: NM 101FluGgp) to label Fluorogold. After 3x PBS washes the following morning (1-2 min each), we used a secondary antibody solution with Alexa Fluor 488 donkey anti-guinea-pig (1:500), Cy3-conjugated anti-goat (1:1000) and Cy5-conjugated anti-rabbit (1:500) for 2 hours. All secondaries antibodies were purchased from Jackson ImmunoResearch (West Grove, PA).

To analyze injection sites in rats, we labeled CTb and HSD2 as described previously (Geerling & Loewy, 2006a; Geerling et al., 2010). After reviewing injection sites in rats, two

cases with CTb injections centered over the HSD2-neuron-containing region of the medial NTS subdivision were chosen for full-brain analysis.

Nissl counterstaining.

After brightfield, whole-slide imaging (see below), we removed coverslips from DAB-stained sections by immersing them in xylenes overnight. We dipped slides for 1 min in a graded series of alcohols with descending concentrations to rehydrate the tissue, then rinsed them in ddH_2O. Then, we submerged slides in a filtered solution of 0.125% thionin (Fisher Scientific) for up to 60 s. Next, we rinsed the slides with tap water until the solution cleared, then dehydrated serially in 50% then 70% EtOH, a fresh 400 mL solution of 95% EtOH with ten drops of glacial acetic acid to clear excess thionin, then 95%, 100%, and 100% EtOH, followed by two incubations in xylenes, after which we coverslipped each slide with Cytoseal. Immunohistochemical DAB labeling and Nissl-counterstaining of rat tissue sections, using similar protocols, were performed prior to whole-slide imaging (for details, see Geerling & Loewy, 2006a; Geerling et al., 2010).

In situ hybridization.

To perform RNAscope, we mounted slides tissue slices containing the hypothalamus and amygdala on glass slides and left them to dry overnight. We used the Multiplex Detection kit (Advanced Cell Diagnostics, Newark, CA) to label mRNA for vesicular glutamate transporter 2 (*Slc17a6)* or the vesicular GABA transporter (*Slc32a1*) in PVH and amygdala, respectively. As a positive control, we labeled *Ubc*. Sections were outlined using a Super-HI PAP pen (Research Products Incorporated) and vacuum grease (Dow Corning) to form a hydrophobic barrier, then we washed sections with PBS 2 x 2 minutes at a room temperature. Then, we incubated the slices with Protease IV in glass petri dishes floating in a 40 °C water bath for 30 min and washed with PBS 2 x 2 minutes. Next, we incubated sections in combinations of probes from Table 2 for 2 hours at 40 °C. After that, we incubated slides in AMP1-4-FL for 15-30 min each at 40°C and washed with RNAscope wash buffer diluted 1:50 in ddH_2O (ref 320058, lot# 2001175) 2x2 min between steps.

After finishing the RNAscope protocol, we washed the slides with PBS and performed an immunofluorescence protocol to label CTb. We dropped a primary antibody solution containing rabbit anti-CTb (1:10.000; Meridian Life Science B65927R, lot # 4D09716) onto each section and incubated overnight at 4 °C. Slides were washed with PBS next morning and incubated with Cy3-conjugated anti-rabbit (1:500; Jackson, ImmunoResearch West Grove, PA) for 2 hours at RT. Finally, we washed the slides in PBS and coverslipped with Vectashield with DAPI.

Image acquisition, figures, plots, and counting.

All sections were imaged and analyzed using a slide-scanning microscope (VS120, Olympus) equipped with a color camera for brightfield imaging (Pike F-505C VC50, Allied Systems), grayscale camera for fluorescence imaging (ORCA-Flash 4.0 C11440, Hamamatsu), and digital imaging software (VS-ASW-S6). Images were acquired as individual stacks using, first, a 10x (NA 0.40) objective for CTb injection sites in the NTS. We then obtained brightfield extended-focal imaging (EFI) using a 20x (NA 0.75) objective

and 13 μm stack thickness to analyze DAB retrogradely labeled cells. Brightfield (DAB-labeled) mouse tissue imaged in this way before and after Nissl-counterstaining (see above), while rat tissue was imaged only after Nissl-counterstaining. In select regions, we also used a 40x (NA 0.95) objective to obtain high-magnification EFI images (11 μm stack thickness) for figures. We imaged Fluorogold i.p.- and CTb-retrogradely labeled neurons in the PVN, *in situ* hybridization, and retrogradely labeled neurons produced by double injections in the NTS using a 20x objective and fluorescence EFI encompassing 3 z-planes through the tissue section.

Grayscale fluorescence images were exported to Adobe Photoshop, and placed into color channels for each labeled tracer or protein. Brightfield images were opened in Photoshop (to adjust color balance, brightness, and contrast) and then masked and arranged in Illustrator for figure layouts. For mouse tissue, whole-slide images before and after Nissl-counterstaining were aligned in separate layers in Adobe Illustrator; for rat tissue, imaging was performed only after Nissl-counterstaining. Then, in additional layers, we used cytoarchitectural landmarks to outline sections and illustrate major white matter tracts. Next, we plotted individual, CTb-containing (DAB-labeled) neurons using the Symbols tool in Illustrator. Scalebars were traced atop calibrated lines in the source images exported from OlyVIA/VS-ASW.

To assess the relative abundance of CTb retrograde labeling across several regions, we reviewed whole-slide images at full-resolution (EFI 20x) and used the counting tool in Cellsens (Olympus). In five CTb-injected brains that were free of histologic artifacts in all regions, we demarcated the ipsilateral rNTS, Rt, PSTN, PVH, CeA, and BST (in two consecutive sections each), the bilateral IC in two consecutive sections (at and immediately rostral to the decussation of the anterior commissure), and the ipsilateral Bar in one section. We used conservative criteria, counting only cells that were in-focus and that contained strong and sharply demarcated DAB labeling (immunohistochemical staining for CTb) in the cytoplasm of the cell soma (and typically in one or more dendrites as well). We then calculated the mean and standard deviation for each region. We did not use the Abercrombie correction factor or any other geometric counting correction because the only variable of interest for these counts was the relative abundance of labeling among brain regions, not the actual number of CTb-labeled cells.

Results

Central afferents to the medial NTS in rats.

Injecting CTb into the NTS produced a consistent pattern of retrograde labeling in both rat brains. Figure 1 shows the whole-brain distribution of retrogradely labeled neurons in rat #8148. The site of injection, shown previously, was centered in the medial NTS with involvement of the dorsal vagal motor nucleus and area postrema (Geerling & Loewy, 2006a; Geerling et al., 2010).

In the hindbrain, just rostral to the site of injection, many neurons were labeled at intermediate and rostral levels of the NTS (Figure 1c-d; Figure 2a). Ventrolateral to the NTS, moderately dense CTb retrograde labeling extended through the reticular formation, and into

the ventrolateral medulla (Figure 1c), which also contained dense CTb labeling in axons (not shown). The paratrigeminal nucleus contained a cluster of retrogradely labeled neurons (Figure 1b). Rostrally, a moderately dense population of CTb-labeled neurons continued through the reticular formation past the facial nerve (Figure 1e-g; Figure 2b-c), ending rostrally beneath the locus coeruleus (Figure 1h). Smaller numbers of retrogradely labeled neurons were present in the parapyramidal region, raphe, and ventromedial medulla (Figure 1a-i).

Further rostrally, Barrington's nucleus contained a small number of densely CTb-labeled neurons (Figure 1i; Figure 2d), and the Kölliker-Fuse nucleus contained moderate number of retrogradely labeled neurons as well (Figure 1j; Figure 2h-i). Fewer, scattered neurons were labeled in the parabrachial nucleus, which instead contained dense, anterograde labeling in axons (not shown). The periaqueductal gray matter contained retrogradely labeled neurons at all rostrocaudal levels, with a stronger concentration in the ventrolateral subdivision (Figure 1j-l). Fewer, scattered neurons were also present throughout the mesencephalic reticular formation (Figure 1k-l).

Rostral to the midbrain, CTb retrograde labeling concentrated in four regions of the forebrain: hypothalamus, central nucleus of the amygdala (CeA), bed nucleus of the stria terminalis (BST), and the cerebral cortex.

In the hypothalamus, the paraventricular nucleus (PVH) contained many, densely CTb-labeled neurons (Figure 1s; Figure 2j). This dense cluster continued laterally through the forniceal PVH (Figure 1q) and into a contiguous region of the lateral hypothalamic area (LHA, Figure 1p-q). Caudal to that, bordering the internal capsule at the midbrain-diencephalic junction, the parasubthalamic nucleus (PSTN) contained CTb retrograde labeling comparable in density to the PVH (Figure 1m; Figure 2g). Outside these nuclei, fewer neurons were labeled in the dorsomedial, arcuate, and tuberomammillary hypothalamic nuclei and medial preoptic area.

In the CeA (Figure 1o-r), the medial subdivision contained many retrogradely labeled neurons (Figure 2f), with fewer in the lateral subdivision. Immediately rostral to the CeA, a moderate number of CTb-labeled neurons extended medially into the sublenticular substantia innominata (Figure 1s-t), including a region referred to as the interstitial nucleus of the posterior limb of the anterior commissure (IPAC; Shammah-Lagnado et al., 2001). Just rostral to this, the dorsal BST contained many retrogradely labeled neurons, with dense CTb labeling just caudal to the oval subnucleus (Figure 1v; Figure 2e). The ventral BST had very few retrogradely labeled neurons, and instead contained a dense cluster of anterogradely labeled axons overlapping the fusiform subnucleus (not shown).

Retrograde labeling in the cerebral cortex concentrated in two limbic areas. The insular cortex (IC) contained CTb-labeled pyramidal neurons in layer 5 (Figure 2k). These neurons were densest in the ipsilateral cortex, at the level of the anterior commissure decussation, but their distribution extended caudally through brain levels containing the caudal BST (Figure 1u-v). Rostral to the anterior commissure decussation, ipsilateral labeling tapered and moderately dense CTb labeling appeared in the contralateral IC, continuing rostrally past the

genu of the corpus callosum (Figure 1y-cc). Just rostral to this, the medial prefrontal cortex contained a moderately dense collection of CTb-labeled neurons ventrally, in the infralimbic area (ILC, Figure 1cc-dd).

Central afferents to the medial NTS in mice.

Collectively, our injection sites in mice covered a large extent of the medial NTS subdivision near the area postrema, with involvement of the dorsal vagal motor nucleus in some cases (Figure 3). In every case, we analyzed the full-brain distribution of CTb retrograde labeling, which is exemplified by a case with an injection site centered in the medial NTS (case #00381). Retrograde labeling in this case is illustrated in Figure 4, with photomicrographs from select brain regions shown in Figure 5.

All cases with CTb injections into the medial NTS had the same overall pattern of retrograde labeling. As in rats, the most prominent collections of retrogradely labeled neurons were in the rostral NTS, reticular formation, hypothalamus, and CeA. Retrograde labeling in these and other brain regions was similar to that in rats in that, despite case-to-case variance in the number or density of CTb labeling, the same brain regions contained labeling in each case. Mice also had sparse retrograde labeling of neurons in the Edinger-Westphal nucleus (Figure 4i), as in rats (not shown). Table 3 shows the relative numbers of CTb-labeled neurons among eight brain regions with consistently heavy labeling across n=5 cases with CTb injections centered in the medial NTS.

One difference in mice was the presence of CTb retrograde labeling in the motor cortex (Figure 4o-q), which was not present in our rat cases. This may have resulted from dorsal spread of CTb pressure injections into the gracile nucleus, which receives heavy input from the motor cortex (Kuypers & Tuerk, 1964), or from CTb entry into axons of passage through this region (Chen & Aston-Jones, 1995). Unlike the NTS, the gracile nucleus projects axons to the ventroposterior lateral nucleus of the thalamus, and indeed this thalamic region contained a small patch of anterograde labeling in all mouse cases (not shown).

PVH afferents to the mouse NTS.

The PVH contains several populations of neuroendocrine neurons, which regulate pituitary hormone release by projecting their axons to the median eminence or neurohypophysis. We injected a subset of mice with intraperitoneal Fluorogold, in addition to CTb in the NTS (n=2), to determine whether the mouse NTS receives axon-collateral projections from any neuroendocrine neurons within the PVH. In these mice, Fluorogold-labeled (neuroendocrine) neurons concentrated in the rostral PVH, with fewer scattered caudally, through the periventricular region (Figure 6a-d). CTb-labeled (NTS-projecting) neurons formed a separate subpopulation at more caudal levels of the PVH (Figure 6b-d). No neurons were double-labeled with CTb and Fluorogold.

Fast neurotransmitter identity of NTS afferents.

To determine the fast neurotransmitter identity of neurons that provide input to the NTS, we performed fluorescence *in situ* hybridization for the vesicular transporters for GABA (Vgat/*Slc32a1*, n=2) or glutamate (Vglut2/*Slc17a6*, n=1) and immunolabeled CTb in the

hypothalamus and amygdala. In the PVH and LHA, all retrogradely labeled neurons expressed *Vglut2* (Figure 7a-d) and lacked *Vgat*. Conversely, in the CeA, all retrogradely labeled neurons expressed *Vgat* (Figure 7e-h) and lacked *Vglut2*.

Afferents to medial and lateral NTS subdivisions.

To explore the possibility that separate brain regions, or separate neurons in the same brain regions, project axons to the medial versus lateral NTS subdivision, we injected two different tracers in three additional cases (Figure 3b). We made non-overlapping injections of CTb into the medial NTS subdivision (and DMV) and Fluorogold into the lateral NTS subdivision (and overlying gracile nucleus) in three mice. Many neurons in the PVH and other afferent brain regions were double-retrogradely labeled with CTb and Fluorogold (Figure 8). In each region, some intermingled neurons were labeled with only CTb or Fluorogold, but the distribution of retrograde labeling was similar for both tracers; neither labeled a spatially distinct cluster of neurons in any afferent site.

Discussion

By comparing afferents to the medial subdivision of the caudal NTS, we find similar patterns of retrograde labeling in mice and rats. Figure 9 shows this overall pattern in the mouse brain. Also, we find that the medial and lateral NTS subdivisions receive input from a similar distribution of retrogradely labeled neurons and show that afferent neurons in the hypothalamus are excitatory (glutamatergic), while those in the amygdala are inhibitory (GABAergic). In the PVH, similar to previous reports in rats and mice (Biag et al., 2012; Swanson et al., 1980), we find that neuroendocrine neurons are distinct from those that project axons to the NTS.

The NTS is an important site for cardiovascular, gastrointestinal, respiratory, and other behavioral responses. Gustatory and other visceral information reaches the NTS from the facial (VII), glossopharyngeal (IX), and vagus (X) nerves to modulate and integrate signals that influence ingestive behavior.

In particular, the aldosterone-sensitive HSD2 neurons in the medial NTS drive the craving for salt after sodium deprivation (Jarvie & Palmiter, 2017; Resch et al., 2017). They are activated by experimental conditions that stimulate sodium appetite, including dietary sodium deprivation and aldosterone infusion into the fourth ventricle (Gasparini et al., 2018; Geerling & Loewy, 2007). Beyond sodium appetite, in both rodents and humans sodium deprivation and elevated aldosterone cause adverse changes in mood, including anhedonia, fatigue, anxiety, and depression (August et al., 1958; Bou-Holaigah et al., 1995; Grippo et al., 2006; Hlavacova et al., 2012; Malinow & Lion, 1979; McCance, 1936; Morris et al., 2006; Reincke, 2018; Sonino et al., 2011). Because the HSD2 neurons in the NTS are the only cells in the brain known to be sensitive to aldosterone, they may mediate the effects of this hormone (and of sodium deprivation) on mood, and the caudal NTS may be a key brain region for peripheral neuroendocrine and viscerosensory changes to alter the activity of forebrain limbic networks that represent emotional states. Identifying afferents to the caudal NTS, therefore, is important for understanding the descending influences over aldosterone-induced mood symptoms in patients with hypovolemia or hyperaldosteronism.

Comparison with prior work on NTS afferents.

In rats, previous retrograde tracing studies have identified an afferent pattern similar to the one shown here (Beckman & Whitehead, 1991; Geerling & Loewy, 2006a; Geerling et al., 2010; Herbert et al., 1990; Krukoff et al., 1993; Ross et al., 1981; Schaffar et al., 1988; Sofroniew, 1983; Spray & Bernstein, 2004; Terenzi & Ingram, 1995; Thor & Helke, 1988; Torrealba & Muller, 1996; van der Kooy et al., 1984; Whitehead et al., 2000).

Also in rats, retrograde labeling in most of these regions was complemented by anterograde axonal labeling in the NTS after tracer injections in the medial prefrontal cortex (Gabbott et al., 2007; Hurley et al., 1991; Terreberry & Neafsey, 1983), insular cortex (Torrealba & Muller, 1996), BST (Dong, Petrovich, Watts, et al., 2001), PVH (Geerling et al., 2010; Luiten et al., 1985; Saper et al., 1976; Toth et al., 1999; Zheng et al., 1995), LHA (Allen & Cechetto, 1992; Berk & Finkelstein, 1982; Kelly & Watts, 1998), PSTN (Goto & Swanson, 2004), IPAC (Shammah-Lagnado et al., 2001), CeA (Danielsen et al., 1989; Geerling & Loewy, 2006a; Schwaber et al., 1982; Zseli et al., 2018), Barrington's nucleus (Valentino et al., 1994), EW (Dos Santos Junior et al., 2015), KF (Geerling et al., 2017; Herbert et al., 1990; Song et al., 2012), and the medullary reticular formation (Herbert et al., 1990). One exception, where anterograde tracing does not produce axonal labeling in the NTS, is the motor cortex. From classic axonal degeneration in cats (Kuypers & Tuerk, 1964) through more recent, publicly available viral tracing data in mice (Oh et al., 2014), anterograde tracing results clearly show that projections from this region of the cerebral cortex target the overlying dorsal column nuclei (gracile and cuneate), not the NTS.

In contrast to the abundance of published data in rats, less was known about afferent projections to the NTS in mice. One study in mice (Ganchrow et al., 2014) examined the brainstem connectivity of a rostral, gustatory region of the NTS, but did not show any brain regions rostral to the medulla.

Functions of central NTS afferents.

We know relatively little about which NTS neurons receive synaptic input from each afferent brain region, or how they integrate this information with other inputs to modify appetite, autonomic reflexes, or other behaviors that are controlled by various subpopulations of neurons within the NTS. The NTS contains a diverse array of interneurons and principal neurons (Kawai & Senba, 1996, 1999). Some receive synaptic input directly from the vagus nerve and control autonomic reflexes via direct output to the ventral medulla (Bailey et al., 2006). Other, larger NTS neurons receive complex information from local interneurons (with little and often no direct vagal input) and project their axons to rostral brain regions, including the PVH (Bailey et al., 2006).

Axonal tracing studies have identified output projections from the NTS to a variety of regions in the upper brainstem and forebrain (Gasparini et al., 2019; Geerling & Loewy, 2006b; Herbert et al., 1990; Kawai, 2018; Ricardo & Koh, 1978; Ter Horst et al., 1989). Prominent targets include the parabrachial nucleus (Herbert et al., 1990; Herbert & Saper, 1990), ventrolateral periaqueductal gray matter (Kawai, 2018), hypothalamus (Ter Horst et

al., 1989), CeA, and ventrolateral BST (Bienkowski & Rinaman, 2013; Geerling & Loewy, 2006b; Ricardo & Koh, 1978; Shin et al., 2008; Sofroniew, 1983; Terenzi & Ingram, 1995).

In both rats and mice, NTS projections to the ventrolateral BST emerge prominently from the aldosterone-sensitive HSD2 neurons (Gasparini et al., 2019; Geerling & Loewy, 2006b; Jarvie & Palmiter, 2017; Resch et al., 2017; Shin et al., 2008). The HSD2 neurons promote sodium appetite via their output projections to the ventrolateral BST (Resch et al., 2017), in a region where neuronal unit activity tracks the reward value of the taste of salt (Tindell et al., 2006) and where lesions and optogenetic inhibition can reduce sodium appetite and salt-seeking behaviors in rats (Chang et al., 2017; Zardetto-Smith et al., 1994). The BST interconnects with the CeA (Dong, Petrovich, & Swanson, 2001; Dong, Petrovich, Watts, et al., 2001), which sends dense axonal projections to the NTS in all mammals studied, including monkeys (Price & Amaral, 1981). In rats, this CeA projection to the NTS massively targets the proximal dendrites and somata of HSD2 neurons (Geerling & Loewy, 2006a).

We confirm here that NTS afferent neurons in the CeA are GABAergic (express the vesicular GABA transporter, *Slc32a1*), consistent with proximal location of CeA axon terminals along the somata and dendrites of HSD2 neurons (Geerling & Loewy, 2006a). Our findings suggest that input from the CeA inhibits HSD2 neurons (and any other post-synaptic targets in the NTS). It remains unclear what role this input plays in modulating sodium appetite and other behaviors, and further work is needed to determine whether HSD2 neurons receive functional synaptic input from other NTS afferent site identified here. For example, their region of the NTS also receives substantial input from the LHA, where bilateral lesions reduce sodium appetite in rats (Dayawansa et al., 2011).

The NTS is important for a broad spectrum of other homeostatic functions including taste, gastrointestinal motility, vomiting, baroreflex control of heart rate and blood pressure, carotid body chemosensory function, and breathing (Cutsforth-Gregory & Benarroch, 2017). The molecular-genetic identities of NTS neuron subtypes that control most of these functions remain unknown, and with few exceptions it is unclear how central afferents to the NTS interact with each cell type and circuit function.

Previous investigators identified NTS neurons that receive vagal, mechanosensory input from the stomach and integrate this information with direct, descending input from the PVH (Banks & Harris, 1987; Rogers & Hermann, 1985). PVH stimulation in these studies was uniformly excitatory, consistent with evidence here and a previous report (Stocker et al., 2006) demonstrating that brainstem-projecting PVH neurons are glutamatergic (express *Slc17a6*). However, another study failed to identify synaptic connectivity from the PVH to all but 7% of NTS glutamatergic neurons they recorded in an *ex vivo* brainstem slice preparation (Shah et al., 2014). The authors concluded that the dense thicket of PVH axons in the NTS (Geerling et al., 2010) primarily target the dendrites of underlying neurons in the DMV, but their finding could also suggest that the PVH targets a select subpopulation of NTS neurons.

The PSTN is another hypothalamic nucleus comprised of glutamatergic neurons that send dense axonal projections to the NTS, as confirmed here in both rats and mice. Stimulating the PSTN in rats evokes potent cardiovascular changes (bradycardia, hypotension, and reduced renal sympathetic nerve activity), possibly by augmenting the activity of baroreflex neurons in the NTS (Ciriello et al., 2008). PSTN neurons that project axons to the NTS receive dense, excitatory input from the insular cortex and inhibitory input from the CeA, suggesting that the insula and CeA exert indirect effects, relayed through the PSTN, in addition to their direct projections to the NTS (Cechetto & Chen, 1990; Tsumori, Yokota, Kishi, et al., 2006; Tsumori, Yokota, Qin, et al., 2006).

The cerebral cortex contains another interesting set of NTS afferents. Neurons that project to the NTS are distributed in two limbic cortical regions – the insular cortex and infralimbic area of the medial prefrontal cortex (Gabbott et al., 2007; Hurley et al., 1991; Terreberry & Neafsey, 1983; Torrealba & Muller, 1996). These regions of the cerebral cortex are considered visceral sensory and motor hubs because they mediate perception of and responses to a variety of changes associated with the internal body state (Craig, 2002). Visceral sensations from the throat, chest, and abdomen are communicated to the brain by the glossopharyngeal and vagus nerves, which synapse in the NTS. Some NTS neurons forward this information rostrally, via multisynaptic pathways to the forebrain, while others control autonomic reflexes via output projections directly to parasympathetic motor neurons in the underlying DMV or nucleus ambiguus, or to pre-sympathetic neurons in the ventrolateral medulla (Cutsforth-Gregory & Benarroch, 2017). The NTS is therefore an ideal site for cortical neurons to modulate visceral sensory and motor functions. Indeed, stimulating the insular cortex in humans produces subjective sensations in the throat, chest, and abdomen as well as changes in gastric motility and breathing (Penfield & Faulk, 1955), and stimulating the medial prefrontal cortex potently decreases blood pressure (Lacuey et al., 2018).

In these same areas of the human cerebral cortex, brain activity increases during several types of emotional experience, ranging from lust to disgust, suggesting that these limbic areas bind emotional states to changes in visceral sensations and visceral motor function (Craig, 2002). The close neurologic association between visceral phenomena and emotional experience has led to ideas ranging from the James-Lange theory of emotion to the somatic marker hypothesis of Damasio (Cannon, 1987; Damasio, 1996). Viral, transneuronal tracing identified the NTS as one of the few sites containing neurons with multisynaptic output connections to both the autonomic nervous system and infralimbic area of the medial prefrontal cortex (Krout et al., 2005), which in humans exhibits prominently abnormal activity in patients with mood disorders (Drevets et al., 1997) and where deep brain stimulation has an immediate, positive impact on mood (Mayberg et al., 2005). Vagus nerve stimulation also is used clinically to improve mood in patients with treatment-resistant depression (Elger et al., 2000; Nahas et al., 2005). These and other lines of evidence, combined with the present findings, highlight the NTS as a key node in the “mind-body” symptoms of several medical and psychiatric diseases (Khalsa et al., 2018; McCance, 1936).

Conclusion.

We describe central afferents to the NTS in rats and mice, characterizing major afferent populations in the hypothalamus and amygdala. This information will help focus future work on central modulation of viscerosensory information. Descending, modulatory input may be important for interoceptive symptoms such as gastrointestinal distress, hyperventilation, chronic pain, or fatigue that are associated with depression and anxiety.

Other Acknowledgements

We thank the late Dr. Arthur Loewy for sharing whole-brain rat CTb tracing results and for mentorship and advice.

Grant sponsors:

NIH K08 NS099425 (JCG)

Aging Mind and Brain Initiative, University of Iowa (JCG)

Data Availability Statement

The data that support the findings of this study are available from the corresponding author upon reasonable request.

List of Abbreviations

7n	facial (7th cranial) nerve
ac	anterior commissure
Bar	Barrington's nucleus
BBB	blood-brain barrier
BST	bed nucleus of the stria terminalis
CeA	central nucleus of the amygdala
CTb	cholera toxin β-subunit
DAB	diaminobenzidine
DMH	dorsomedial hypothalamic nucleus
EW	Edinger-Westphal nucleus
g7	genu of the facial (7th cranial) nerve
HSD2	11-β-hydroxysteroid dehydrogenase 2
IC	insular cortex
ILC	Infralimbic cortex
i.p.	intraperitoneal

KF	Kölliker-Fuse nucleus
LHA	lateral hypothalamic area
NTS	nucleus of the solitary tract
opt	optic tract
Pa5	paratrigeminal nucleus
PAG	periaqueductal gray matter
PBS	phosphate-buffered saline
PPR	parapyramidal
PSTN	parasubthalamic nucleus
PVH	paraventricular hypothalamic nucleus
rNTS	rostral subdivision of the NTS
ROb	raphe obscurus
Rt	reticular formation
SI	substantia innominata
VLM	ventrolateral medulla

References

Allen GV, & Cechetto DF (1992, 1 15). Functional and anatomical organization of cardiovascular pressor and depressor sites in the lateral hypothalamic area: I. Descending projections. J Comp Neurol, 315(3), 313–332. 10.1002/cne.903150307 [PubMed: 1740546]

Altschuler SM, Ferenci DA, Lynn RB, & Miselis RR (1991, 2 8). Representation of the cecum in the lateral dorsal motor nucleus of the vagus nerve and commissural subnucleus of the nucleus tractus solitarii in rat. J Comp Neurol, 304(2), 261–274. 10.1002/cne.903040209 [PubMed: 1707898]

August JT, Nelson DH, & Thorn GW (1958, 11). Response of normal subjects to large amounts of aldosterone. J Clin Invest, 37(11), 1549–1555. 10.1172/JCI103747 [PubMed: 13587664]

Bailey TW, Hermes SM, Andresen MC, & Aicher SA (2006, 11 15). Cranial visceral afferent pathways through the nucleus of the solitary tract to caudal ventrolateral medulla or paraventricular hypothalamus: target-specific synaptic reliability and convergence patterns. J Neurosci, 26(46), 11893–11902. 10.1523/JNEUROSCI.2044-06.2006 [PubMed: 17108163]

Banks D, & Harris MC (1987, 5). Activation within dorsal medullary nuclei following stimulation in the hypothalamic paraventricular nucleus in rats. Pflugers Arch, 408(6), 619–627. 10.1007/bf00581165 [PubMed: 3601646]

Barnett WH, Abdala AP, Paton JF, Rybak IA, Zoccal DB, & Molkov YI (2017, 1). Chemoreception and neuroplasticity in respiratory circuits. Exp Neurol, 287(Pt 2), 153–164. 10.1016/j.expneurol.2016.05.036 [PubMed: 27240520]

Beckman ME, & Whitehead MC (1991, 8 23). Intramedullary connections of the rostral nucleus of the solitary tract in the hamster. Brain Res, 557(1-2), 265–279. 10.1016/0006-8993(91)90143-j [PubMed: 1747757]

Berk ML, & Finkelstein JA (1982, 5). Efferent connections of the lateral hypothalamic area of the rat: an autoradiographic investigation. Brain Res Bull, 8(5), 511–526. [PubMed: 6811106]

Biag J, Huang Y, Gou L, Hintiryan H, Askarinam A, Hahn JD, Toga AW, & Dong HW (2012, 1 1). Cyto- and chemoarchitecture of the hypothalamic paraventricular nucleus in the C57BL/6J male mouse: a study of immunostaining and multiple fluorescent tract tracing. J Comp Neurol, 520(1), 6–33. 10.1002/cne.22698 [PubMed: 21674499]

Bienkowski MS, & Rinaman L (2013, 1). Common and distinct neural inputs to the medial central nucleus of the amygdala and anterior ventrolateral bed nucleus of stria terminalis in rats. Brain Struct Funct, 218(1), 187–208. 10.1007/s00429-012-0393-6 [PubMed: 22362201]

Bonham AC, & McCrimmon DR (1990, 8). Neurones in a discrete region of the nucleus tractus solitarius are required for the Breuer-Hering reflex in rat. J Physiol, 427, 261–280. [PubMed: 2213599]

Bou-Holaigah I, Rowe PC, Kan J, & Calkins H (1995, 9 27). The relationship between neurally mediated hypotension and the chronic fatigue syndrome. JAMA, 274(12), 961–967. [PubMed: 7674527]

Cannon WB (1987, Fall-Winter). The James-Lange theory of emotions: a critical examination and an alternative theory. By Walter B. Cannon, 1927. Am J Psychol, 100(3-4), 567–586. [PubMed: 3322057]

Cechetto DF, & Chen SJ (1990, 1). Subcortical sites mediating sympathetic responses from insular cortex in rats. Am J Physiol, 258(1 Pt 2), R245–255. 10.1152/ajpregu.1990.258.1.R245 [PubMed: 2301638]

Chan RK, Jarvina EV, & Sawchenko PE (2000). Effects of selective sinoaortic denervations on phenylephrine-induced activational responses in the nucleus of the solitary tract. Neuroscience, 101(1), 165–178. 10.1016/s0306-4522(00)00332-8 [PubMed: 11068145]

Chang RB, Strochlic DE, Williams EK, Umans BD, & Liberles SD (2015, 4 23). Vagal Sensory Neuron Subtypes that Differentially Control Breathing. Cell, 161(3), 622–633. 10.1016/j.cell.2015.03.022 [PubMed: 25892222]

Chang SE, Smedley EB, Stansfield KJ, Stott JJ, & Smith KS (2017, 6 7). Optogenetic Inhibition of Ventral Pallidum Neurons Impairs Context-Driven Salt Seeking. J Neurosci, 37(23), 5670–5680. 10.1523/JNEUROSCI.2968-16.2017 [PubMed: 28495976]

Chen S, & Aston-Jones G (1995, 3 13). Evidence that cholera toxin B subunit (CTb) can be avidly taken up and transported by fibers of passage. Brain Res, 674(1), 107–111. [PubMed: 7773677]

Ciriello J (1983, 3 28). Brainstem projections of aortic baroreceptor afferent fibers in the rat. Neurosci Lett, 36(1), 37–42. 10.1016/0304-3940(83)90482-2 [PubMed: 6856201]

Ciriello J, Solano-Flores LP, Rosas-Arellano MP, Kirouac GJ, & Babic T (2008, 4). Medullary pathways mediating the parasubthalamic nucleus depressor response. Am J Physiol Regul Integr Comp Physiol, 294(4), R1276–1284. 10.1152/ajpregu.00437.2007 [PubMed: 18287224]

Contreras RJ, Beckstead RM, & Norgren R (1982, 11). The central projections of the trigeminal, facial, glossopharyngeal and vagus nerves: an autoradiographic study in the rat. J Auton Nerv Syst, 6(3), 303–322. [PubMed: 7169500]

Corbett EK, Sinfield JK, McWilliam PN, Deuchars J, & Batten TF (2005). Differential expression of vesicular glutamate transporters by vagal afferent terminals in rat nucleus of the solitary tract: projections from the heart preferentially express vesicular glutamate transporter 1. Neuroscience, 135(1), 133–145. 10.1016/j.neuroscience.2005.06.010 [PubMed: 16084661]

Craig AD (2002, 8). How do you feel? Interoception: the sense of the physiological condition of the body. Nat Rev Neurosci, 3(8), 655–666. 10.1038/nrn894 [PubMed: 12154366]

Cunningham ET Jr., & Sawchenko PE (1990). Central neural control of esophageal motility: a review. Dysphagia, 5(1), 35–51. [PubMed: 2202557]

Cutsforth-Gregory JK, & Benarroch EE (2017, 3 21). Nucleus of the solitary tract, medullary reflexes, and clinical implications. Neurology, 88(12), 1187–1196. 10.1212/WNL.0000000000003751 [PubMed: 28202704]

Damasio AR (1996, 10 29). The somatic marker hypothesis and the possible functions of the prefrontal cortex. Philos Trans R Soc Lond B Biol Sci, 351(1346), 1413–1420. 10.1098/rstb.1996.0125 [PubMed: 8941953]

Danielsen EH, Magnuson DJ, & Gray TS (1989, 4). The central amygdaloid nucleus innervation of the dorsal vagal complex in rat: a Phaseolus vulgaris leucoagglutinin lectin anterograde tracing study. Brain Res Bull, 22(4), 705–715. 10.1016/0361-9230(89)90090-7 [PubMed: 2736396]

Dayawansa S, Peckins S, Ruch S, & Norgren R (2011, 5). Parabrachial and hypothalamic interaction in sodium appetite. Am J Physiol Regul Integr Comp Physiol, 300(5), R1091–1099. 10.1152/ajpregu.00615.2010 [PubMed: 21270347]

Dong HW, Petrovich GD, & Swanson LW (2001, 12). Topography of projections from amygdala to bed nuclei of the stria terminalis. Brain Res Brain Res Rev, 38(1-2), 192–246. [PubMed: 11750933]

Dong HW, Petrovich GD, Watts AG, & Swanson LW (2001, 8 6). Basic organization of projections from the oval and fusiform nuclei of the bed nuclei of the stria terminalis in adult rat brain. J Comp Neurol, 436(4), 430–455. [PubMed: 11447588]

Dos Santos Junior ED, Da Silva AV, Da Silva KR, Haemmerle CA, Batagello DS, Da Silva JM, Lima LB, Da Silva RJ, Diniz GB, Sita LV, Elias CF, & Bittencourt JC (2015, 10). The centrally projecting Edinger-Westphal nucleus--I: Efferents in the rat brain. J Chem Neuroanat, 68, 22–38. 10.1016/j.jchemneu.2015.07.002 [PubMed: 26206178]

Drevets WC, Price JL, Simpson JR Jr., Todd RD, Reich T, Vannier M, & Raichle ME (1997, 4 24). Subgenual prefrontal cortex abnormalities in mood disorders. Nature, 386(6627), 824–827. 10.1038/386824a0 [PubMed: 9126739]

Elger G, Hoppe C, Falkai P, Rush AJ, & Elger CE (2000, 12). Vagus nerve stimulation is associated with mood improvements in epilepsy patients. Epilepsy Res, 42(2-3), 203–210. 10.1016/s0920-1211(00)00181-9 [PubMed: 11074193]

Finley JC, & Katz DM (1992, 2 14). The central organization of carotid body afferent projections to the brainstem of the rat. Brain Res, 572(1-2), 108–116. [PubMed: 1611506]

Gabbott PL, Warner T, & Busby SJ (2007, 1 19). Catecholaminergic neurons in medullary nuclei are among the post-synaptic targets of descending projections from infralimbic area 25 of the rat medial prefrontal cortex. Neuroscience, 144(2), 623–635. 10.1016/j.neuroscience.2006.09.048 [PubMed: 17101227]

Ganchrow D, Ganchrow JR, Cicchini V, Bartel DL, Kaufman D, Girard D, & Whitehead MC (2014, 5 1). Nucleus of the solitary tract in the C57BL/6J mouse: Subnuclear parcellation, chorda tympani nerve projections, and brainstem connections. J Comp Neurol, 522(7), 1565–1596. 10.1002/cne.23484 [PubMed: 24151133]

Gasparini S, Melo MR, Andrade-Franze GMF, Geerling JC, Menani JV, & Colombari E (2018, 6 18). Aldosterone infusion into the 4(th) ventricle produces sodium appetite with baroreflex attenuation independent of renal or blood pressure changes. Brain Res. 10.1016/j.brainres.2018.06.023

Gasparini S, Resch JM, Narayan SV, Peltekian L, Iverson GN, Karthik S, & Geerling JC (2019, 1). Aldosterone-sensitive HSD2 neurons in mice. Brain Struct Funct, 224(1), 387–417. 10.1007/s00429-018-1778-y [PubMed: 30343334]

Geerling JC, Engeland WC, Kawata M, & Loewy AD (2006, 1 11). Aldosterone target neurons in the nucleus tractus solitarius drive sodium appetite. J Neurosci, 26(2), 411–417. https://doi.org/26/2/411 [pii] 10.1523/JNEUROSCI.3115-05.2006 [PubMed: 16407537]

Geerling JC, Kawata M, & Loewy AD (2006, 1 20). Aldosterone-sensitive neurons in the rat central nervous system. J Comp Neurol, 494(3), 515–527. 10.1002/cne.20808 [PubMed: 16320254]

Geerling JC, & Loewy AD (2006a, 8 1). Aldosterone-sensitive neurons in the nucleus of the solitary tract: bidirectional connections with the central nucleus of the amygdala. J Comp Neurol, 497(4), 646–657. 10.1002/cne.21019 [PubMed: 16739197]

Geerling JC, & Loewy AD (2006b, 9 20). Aldosterone-sensitive neurons in the nucleus of the solitary: efferent projections. J Comp Neurol, 498(3), 223–250. [PubMed: 16933386]

Geerling JC, & Loewy AD (2007, 3). Sodium depletion activates the aldosterone-sensitive neurons in the NTS independently of thirst. Am J Physiol Regul Integr Comp Physiol, 292(3), R1338–1348. https://doi.org/00391.2006 [pii] 10.1152/ajpregu.00391.2006 [PubMed: 17068161]

Geerling JC, Shin JW, Chimenti PC, & Loewy AD (2010, 5 1). Paraventricular hypothalamic nucleus: axonal projections to the brainstem. J Comp Neurol, 518(9), 1460–1499. 10.1002/cne.22283 [PubMed: 20187136]

Geerling JC, Yokota S, Rukhadze I, Roe D, & Chamberlin NL (2017, 6 1). Kölliker-Fuse GABAergic and glutamatergic neurons project to distinct targets. J Comp Neurol, 525(8), 1844–1860. 10.1002/cne.24164 [PubMed: 28032634]

Goto M, & Swanson LW (2004, 2 16). Axonal projections from the parasubthalamic nucleus. J Comp Neurol, 469(4), 581–607. 10.1002/cne.11036 [PubMed: 14755537]

Grippo AJ, Moffitt JA, Beltz TG, & Johnson AK (2006, 10). Reduced hedonic behavior and altered cardiovascular function induced by mild sodium depletion in rats. Behav Neurosci, 120(5), 1133–1143. 10.1037/0735-7044.120.5.1133 [PubMed: 17014263]

Guyenet PG (2006, 5). The sympathetic control of blood pressure. Nat Rev Neurosci, 7(5), 335–346. https://doi.org/nrn1902 [pii] 10.1038/nrn1902 [PubMed: 16760914]

Hamilton RB, & Norgren R (1984, 2 1). Central projections of gustatory nerves in the rat. J Comp Neurol, 222(4), 560–577. 10.1002/cne.902220408 [PubMed: 6199385]

Hardy SG (2001, 3 16). Hypothalamic projections to cardiovascular centers of the medulla. Brain Res, 894(2), 233–240. 10.1016/s0006-8993(01)02053-4 [PubMed: 11251196]

Herbert H, Moga MM, & Saper CB (1990, 3 22). Connections of the parabrachial nucleus with the nucleus of the solitary tract and the medullary reticular formation in the rat. J Comp Neurol, 293(4), 540–580. 10.1002/cne.902930404 [PubMed: 1691748]

Herbert H, & Saper CB (1990, 3 22). Cholecystokinin-, galanin-, and corticotropin-releasing factor-like immunoreactive projections from the nucleus of the solitary tract to the parabrachial nucleus in the rat. J Comp Neurol, 293(4), 581–598. 10.1002/cne.902930405 [PubMed: 1691749]

Hlavacova N, Wes PD, Ondrejcakova M, Flynn ME, Poundstone PK, Babic S, Murck H, & Jezova D (2012, 3). Subchronic treatment with aldosterone induces depression-like behaviours and gene expression changes relevant to major depressive disorder. Int J Neuropsychopharmacol, 15(2), 247–265. 10.1017/S1461145711000368 [PubMed: 21375792]

Hurley KM, Herbert H, Moga MM, & Saper CB (1991, 6 8). Efferent projections of the infralimbic cortex of the rat. J Comp Neurol, 308(2), 249–276. 10.1002/cne.903080210 [PubMed: 1716270]

Jarvie BC, & Palmiter RD (2017, 2). HSD2 neurons in the hindbrain drive sodium appetite. Nat Neurosci, 20(2), 167–169. 10.1038/nn.4451 nn.4451 [pii] [PubMed: 27918529]

Kalia M, & Mesulam MM (1980, 9 15). Brain stem projections of sensory and motor components of the vagus complex in the cat: II. Laryngeal, tracheobronchial, pulmonary, cardiac, and gastrointestinal branches. J Comp Neurol, 193(2), 467–508. 10.1002/cne.901930211 [PubMed: 7440778]

Kawai Y (2018). Differential Ascending Projections From the Male Rat Caudal Nucleus of the Tractus Solitarius: An Interface Between Local Microcircuits and Global Macrocircuits. Front Neuroanat, 12, 63. 10.3389/fnana.2018.00063 [PubMed: 30087599]

Kawai Y, & Senba E (1996, 9 23). Organization of excitatory and inhibitory local networks in the caudal nucleus of tractus solitarius of rats revealed in in vitro slice preparation. J Comp Neurol, 373(3), 309–321. 10.1002/(SICI)1096-9861(19960923)373:3<309::AID-CNE1>3.0.CO;2-6 [PubMed: 8889930]

Kawai Y, & Senba E (1999). Electrophysiological and morphological characterization of cytochemically-defined neurons in the caudal nucleus of tractus solitarius of the rat. Neuroscience, 89(4), 1347–1355. 10.1016/s0306-4522(98)00393-5 [PubMed: 10362319]

Kelly AB, & Watts AG (1998, 4 27). The region of the pontine parabrachial nucleus is a major target of dehydration-sensitive CRH neurons in the rat lateral hypothalamic area. J Comp Neurol, 394(1), 48–63. 10.1002/(sici)1096-9861(19980427)394:1<48::aid-cne5>3.0.co;2-h [PubMed: 9550142]

Khalsa SS, Adolphs R, Cameron OG, Critchley HD, Davenport PW, Feinstein JS, Feusner JD, Garfinkel SN, Lane RD, Mehling WE, Meuret AE, Nemeroff CB, Oppenheimer S, Petzschner FH, Pollatos O, Rhudy JL, Schramm LP, Simmons WK, Stein MB, Stephan KE, Van den Bergh O, Van Diest I, von Leupoldt A, Paulus MP, & Interoception Summit, p. (2018, 6). Interoception and Mental Health: A Roadmap. Biol Psychiatry Cogn Neurosci Neuroimaging, 3(6), 501–513. 10.1016/j.bpsc.2017.12.004 [PubMed: 29884281]

Krout KE, Mettenleiter TC, Karpitskiy V, Nguyen XV, & Loewy AD (2005, 7 19). CNS neurons with links to both mood-related cortex and sympathetic nervous system. Brain Res, 1050(1-2), 199–202. 10.1016/j.brainres.2005.04.090 [PubMed: 15975562]

Krukoff TL, Harris KH, & Jhamandas JH (1993). Efferent projections from the parabrachial nucleus demonstrated with the anterograde tracer Phaseolus vulgaris leucoagglutinin. Brain Res Bull, 30(1-2), 163–172. [PubMed: 7678381]

Kuypers HG, & Tuerk JD (1964, 4). The Distribution of the Cortical Fibres within the Nuclei Cuneatus and Gracilis in the Cat. J Anat, 98, 143–162. [PubMed: 14154418]

Lacuey N, Hampson JP, Theeranaew W, Zonjy B, Vithala A, Hupp NJ, Loparo KA, Miller JP, & Lhatoo SD (2018, 2 1). Cortical Structures Associated With Human Blood Pressure Control. JAMA Neurol, 75(2), 194–202. 10.1001/jamaneurol.2017.3344 [PubMed: 29181526]

Luiten PG, ter Horst GJ, Karst H, & Steffens AB (1985, 3 11). The course of paraventricular hypothalamic efferents to autonomic structures in medulla and spinal cord. Brain Res, 329(1-2), 374–378. 10.1016/0006-8993(85)90554-2 [PubMed: 3978460]

Malinow KC, & Lion JR (1979, 8). Hyperaldosteronism (Conn's disease) presenting as depression. J Clin Psychiatry, 40(8), 358–359. [PubMed: 468762]

May OL, & Hill DL (2006, 8 1). Gustatory terminal field organization and developmental plasticity in the nucleus of the solitary tract revealed through triple-fluorescence labeling. J Comp Neurol, 497(4), 658–669. 10.1002/cne.21023 [PubMed: 16739199]

Mayberg HS, Lozano AM, Voon V, McNeely HE, Seminowicz D, Hamani C, Schwalb JM, & Kennedy SH (2005, 3 3). Deep brain stimulation for treatment-resistant depression. Neuron, 45(5), 651–660. 10.1016/j.neuron.2005.02.014 [PubMed: 15748841]

McCance RA (1936, 4 11, 1936). Experimental human salt deficiency. Lancet, 1, 823–830.

Menetrey D, & Basbaum AI (1987, 10). The distribution of substance P-, enkephalin- and dynorphin-immunoreactive neurons in the medulla of the rat and their contribution to bulbospinal pathways. Neuroscience, 23(1), 173–187. 10.1016/0306-4522(87)90281-8 [PubMed: 2446203]

Merchenthaler I (1991). Neurons with access to the general circulation in the central nervous system of the rat: a retrograde tracing study with fluoro-gold. Neuroscience, 44(3), 655–662. 10.1016/0306-4522(91)90085-3 [PubMed: 1721686]

Moreira TS, Takakura AC, Colombari E, & Menani JV (2009, 6). Antihypertensive effects of central ablations in spontaneously hypertensive rats. Am J Physiol Regul Integr Comp Physiol, 296(6), R1797–1806. 10.1152/ajpregu.90730.2008 90730.2008 [pii] [PubMed: 19339677]

Morris MJ, Na ES, Grippo AJ, & Johnson AK (2006, 6). The effects of deoxycorticosterone-induced sodium appetite on hedonic behaviors in the rat. Behav Neurosci, 120(3), 571–579. 10.1037/0735-7044.120.3.571 [PubMed: 16768609]

Nahas Z, Marangell LB, Husain MM, Rush AJ, Sackeim HA, Lisanby SH, Martinez JM, & George MS (2005, 9). Two-year outcome of vagus nerve stimulation (VNS) for treatment of major depressive episodes. J Clin Psychiatry, 66(9), 1097–1104. 10.4088/jcp.v66n0902 [PubMed: 16187765]

Norgren R, & Smith GP (1988, 7 8). Central distribution of subdiaphragmatic vagal branches in the rat. J Comp Neurol, 273(2), 207–223. 10.1002/cne.902730206 [PubMed: 3417902]

Oh SW, Harris JA, Ng L, Winslow B, Cain N, Mihalas S, Wang Q, Lau C, Kuan L, Henry AM, Mortrud MT, Ouellette B, Nguyen TN, Sorensen SA, Slaughterbeck CR, Wakeman W, Li Y, Feng D, Ho A, Nicholas E, Hirokawa KE, Bohn P, Joines KM, Peng H, Hawrylycz MJ, Phillips JW, Hohmann JG, Wohnoutka P, Gerfen CR, Koch C, Bernard A, Dang C, Jones AR, & Zeng H (2014, 4 10). A mesoscale connectome of the mouse brain. Nature, 508(7495), 207–214. 10.1038/nature13186 [PubMed: 24695228]

Penfield W, & Faulk ME Jr. (1955). The insula; further observations on its function. Brain, 78(4), 445–470. 10.1093/brain/78.4.445 [PubMed: 13293263]

Price JL, & Amaral DG (1981, 11). An autoradiographic study of the projections of the central nucleus of the monkey amygdala. J Neurosci, 1(11), 1242–1259. [PubMed: 6171630]

Reincke M (2018, 1 1). Anxiety, Depression, and Impaired Quality of Life in Primary Aldosteronism: Why We Shouldn't Ignore It! J Clin Endocrinol Metab, 103(1), 1–4. 10.1210/jc.2017-02141 [PubMed: 29099927]

Resch JM, Fenselau H, Madara JC, Wu C, Campbell JN, Lyubetskaya A, Dawes BA, Tsai LT, Li MM, Livneh Y, Ke Q, Kang PM, Fejes-Toth G, Naray-Fejes-Toth A, Geerling JC, & Lowell BB (2017, 9 27). Aldosterone-Sensing Neurons in the NTS Exhibit State-Dependent Pacemaker Activity and

Drive Sodium Appetite via Synergy with Angiotensin II Signaling. Neuron, 96(1), 190–206 e197. 10.1016/j.neuron.2017.09.014 [PubMed: 28957668]

Ricardo JA, & Koh ET (1978, 9 15). Anatomical evidence of direct projections from the nucleus of the solitary tract to the hypothalamus, amygdala, and other forebrain structures in the rat. Brain Res, 153(1), 1–26. [PubMed: 679038]

Rogers RC, & Hermann GE (1985, 12). Gastric-vagal solitary neurons excited by paraventricular nucleus microstimulation. J Auton Nerv Syst, 14(4), 351–362. 10.1016/0165-1838(85)90081-5 [PubMed: 4086724]

Roman CW, Derkach VA, & Palmiter RD (2016, 6 15). Genetically and functionally defined NTS to PBN brain circuits mediating anorexia. Nat Commun, 7, 11905. 10.1038/ncomms11905 [PubMed: 27301688]

Ross CA, Ruggiero DA, & Reis DJ (1981, 11 2). Afferent projections to cardiovascular portions of the nucleus of the tractus solitarius in the rat. Brain Res, 223(2), 402–408. [PubMed: 6169408]

Saper CB, Loewy AD, Swanson LW, & Cowan WM (1976, 11 26). Direct hypothalamo-autonomic connections. Brain Res, 117(2), 305–312. 10.1016/0006-8993(76)90738-1 [PubMed: 62600]

Schaffar N, Kessler JP, Bosler O, & Jean A (1988, 9). Central serotonergic projections to the nucleus tractus solitarii: evidence from a double labeling study in the rat. Neuroscience, 26(3), 951–958. [PubMed: 3200434]

Schwaber JS, Kapp BS, Higgins GA, & Rapp PR (1982, 10). Amygdaloid and basal forebrain direct connections with the nucleus of the solitary tract and the dorsal motor nucleus. J Neurosci, 2(10), 1424–1438. [PubMed: 6181231]

Sequeira SM, Geerling JC, & Loewy AD (2006, 9 15). Local inputs to aldosterone-sensitive neurons of the nucleus tractus solitarius. Neuroscience, 141(4), 1995–2005. 10.1016/j.neuroscience.2006.05.059 [PubMed: 16828976]

Shah BP, Vong L, Olson DP, Koda S, Krashes MJ, Ye C, Yang Z, Fuller PM, Elmquist JK, & Lowell BB (2014, 9 9). MC4R-expressing glutamatergic neurons in the paraventricular hypothalamus regulate feeding and are synaptically connected to the parabrachial nucleus. Proc Natl Acad Sci U S A, 111(36), 13193–13198. 10.1073/pnas.1407843111 [PubMed: 25157144]

Shammah-Lagnado SJ, Alheid GF, & Heimer L (2001, 10 8). Striatal and central extended amygdala parts of the interstitial nucleus of the posterior limb of the anterior commissure: evidence from tract-tracing techniques in the rat. J Comp Neurol, 439(1), 104–126. 10.1002/cne.1999 [PubMed: 11584811]

Shin JW, Geerling JC, & Loewy AD (2008, 12 10). Inputs to the ventrolateral bed nucleus of the stria terminalis. J Comp Neurol, 511(5), 628–657. 10.1002/cne.21870 [PubMed: 18853414]

Shin JW, Geerling JC, & Loewy AD (2009, 1 16). Vagal innervation of the aldosterone-sensitive HSD2 neurons in the NTS. Brain Res, 1249, 135–147. 10.1016/j.brainres.2008.10.058 [PubMed: 19010311]

Sofroniew MV (1983, 2 1). Direct reciprocal connections between the bed nucleus of the stria terminalis and dorsomedial medulla oblongata: evidence from immunohistochemical detection of tracer proteins. J Comp Neurol, 213(4), 399–405. 10.1002/cne.902130404 [PubMed: 6833532]

Song G, Wang H, Xu H, & Poon CS (2012, 10). Kölliker-Fuse neurons send collateral projections to multiple hypoxia-activated and nonactivated structures in rat brainstem and spinal cord. Brain Struct Funct, 217(4), 835–858. 10.1007/s00429-012-0384-7 [PubMed: 22286911]

Sonino N, Tomba E, Genesia ML, Bertello C, Mulatero P, Veglio F, Fava GA, & Fallo F (2011, 6). Psychological assessment of primary aldosteronism: a controlled study. J Clin Endocrinol Metab, 96(6), E878–883. 10.1210/jc.2010-2723 [PubMed: 21389142]

Spray KJ, & Bernstein IL (2004, 9 23). Afferent and efferent connections of the parvicellular subdivision of iNTS: defining a circuit involved in taste aversion learning. Behav Brain Res, 154(1), 85–97. 10.1016/j.bbr.2004.01.027 [PubMed: 15302114]

Stocker SD, Simmons JR, Stornetta RL, Toney GM, & Guyenet PG (2006, 2 1). Water deprivation activates a glutamatergic projection from the hypothalamic paraventricular nucleus to the rostral ventrolateral medulla. J Comp Neurol, 494(4), 673–685. 10.1002/cne.20835 [PubMed: 16374796]

Swanson LW, Sawchenko PE, Wiegand SJ, & Price JL (1980, 9 29). Separate neurons in the paraventricular nucleus project to the median eminence and to the medulla or spinal cord. Brain Res, 198(1), 190–195. 10.1016/0006-8993(80)90354-6 [PubMed: 7407584]

Ter Horst GJ, de Boer P, Luiten PG, & van Willigen JD (1989). Ascending projections from the solitary tract nucleus to the hypothalamus. A Phaseolus vulgaris lectin tracing study in the rat. Neuroscience, 31(3), 785–797. [PubMed: 2594200]

Terenzi MG, & Ingram CD (1995, 2 20). A combined immunocytochemical and retrograde tracing study of noradrenergic connections between the caudal medulla and bed nuclei of the stria terminalis. Brain Res, 672(1-2), 289–297. [PubMed: 7749750]

Terreberry RR, & Neafsey EJ (1983, 11 14). Rat medial frontal cortex: a visceral motor region with a direct projection to the solitary nucleus. Brain Res, 278(1-2), 245–249. 10.1016/0006-8993(83)90246-9 [PubMed: 6315155]

Thor KB, & Helke CJ (1988, 2 8). Catecholamine-synthesizing neuronal projections to the nucleus tractus solitarii of the rat. J Comp Neurol, 268(2), 264–280. 10.1002/cne.902680210 [PubMed: 3360988]

Tindell AJ, Smith KS, Pecina S, Berridge KC, & Aldridge JW (2006, 11). Ventral pallidum firing codes hedonic reward: when a bad taste turns good. J Neurophysiol, 96(5), 2399–2409. 10.1152/jn.00576.2006 [PubMed: 16885520]

Torrealba F, & Muller C (1996, 3). Glutamate immunoreactivity of insular cortex afferents to the nucleus tractus solitarius in the rat: a quantitative electron microscopic study. Neuroscience, 71(1), 77–87. [PubMed: 8834393]

Toth ZE, Gallatz K, Fodor M, & Palkovits M (1999, 11 15). Decussations of the descending paraventricular pathways to the brainstem and spinal cord autonomic centers. J Comp Neurol, 414(2), 255–266. [PubMed: 10516595]

Tsumori T, Yokota S, Kishi T, Qin Y, Oka T, & Yasui Y (2006, 1 27). Insular cortical and amygdaloid fibers are in contact with posterolateral hypothalamic neurons projecting to the nucleus of the solitary tract in the rat. Brain Res, 1070(1), 139–144. 10.1016/j.brainres.2005.11.040 [PubMed: 16388783]

Tsumori T, Yokota S, Qin Y, Oka T, & Yasui Y (2006, 11). A light and electron microscopic analysis of the convergent insular cortical and amygdaloid projections to the posterior lateral hypothalamus in the rat, with special reference to cardiovascular function. Neurosci Res, 56(3), 261–269. 10.1016/j.neures.2006.07.005 [PubMed: 16935375]

Valentino RJ, Page ME, Luppi PH, Zhu Y, Van Bockstaele E, & Aston-Jones G (1994, 9). Evidence for widespread afferents to Barrington's nucleus, a brainstem region rich in corticotropin-releasing hormone neurons. Neuroscience, 62(1), 125–143. 10.1016/0306-4522(94)90320-4 [PubMed: 7816195]

van der Kooy D, Koda LY, McGinty JF, Gerfen CR, & Bloom FE (1984, 3 20). The organization of projections from the cortex, amygdala, and hypothalamus to the nucleus of the solitary tract in rat. J Comp Neurol, 224(1), 1–24. 10.1002/cne.902240102 [PubMed: 6715573]

Whitehead MC, Bergula A, & Holliday K (2000, 7 3). Forebrain projections to the rostral nucleus of the solitary tract in the hamster. J Comp Neurol, 422(3), 429–447. [PubMed: 10861518]

Williams DL, Lilly NA, Edwards IJ, Yao P, Richards JE, & Trapp S (2018, 3 15). GLP-1 action in the mouse bed nucleus of the stria terminalis. Neuropharmacology, 131, 83–95. 10.1016/j.neuropharm.2017.12.007 [PubMed: 29221794]

Williams EK, Chang RB, Strochlic DE, Umans BD, Lowell BB, & Liberles SD (2016, 6 30). Sensory Neurons that Detect Stretch and Nutrients in the Digestive System. Cell, 166(1), 209–221. 10.1016/j.cell.2016.05.011 [PubMed: 27238020]

Zardetto-Smith AM, Beltz TG, & Johnson AK (1994, 5 9). Role of the central nucleus of the amygdala and bed nucleus of the stria terminalis in experimentally-induced salt appetite. Brain Res, 645(1-2), 123–134. [PubMed: 8062074]

Zheng JQ, Seki M, Hayakawa T, Ito H, & Zyo K (1995, 8). Descending projections from the paraventricular hypothalamic nucleus to the spinal cord: anterograde tracing study in the rat. Okajimas Folia Anat Jpn, 72(2-3), 119–135. 10.2535/ofaj1936.72.2-3_119 [PubMed: 8559555]

Zseli G, Vida B, Szilvasy-Szabo A, Toth M, Lechan RM, & Fekete C (2018, 1). Neuronal connections of the central amygdalar nucleus with refeeding-activated brain areas in rats. Brain Struct Funct, 223(1), 391–414. 10.1007/s00429-017-1501-4 [PubMed: 28852859]

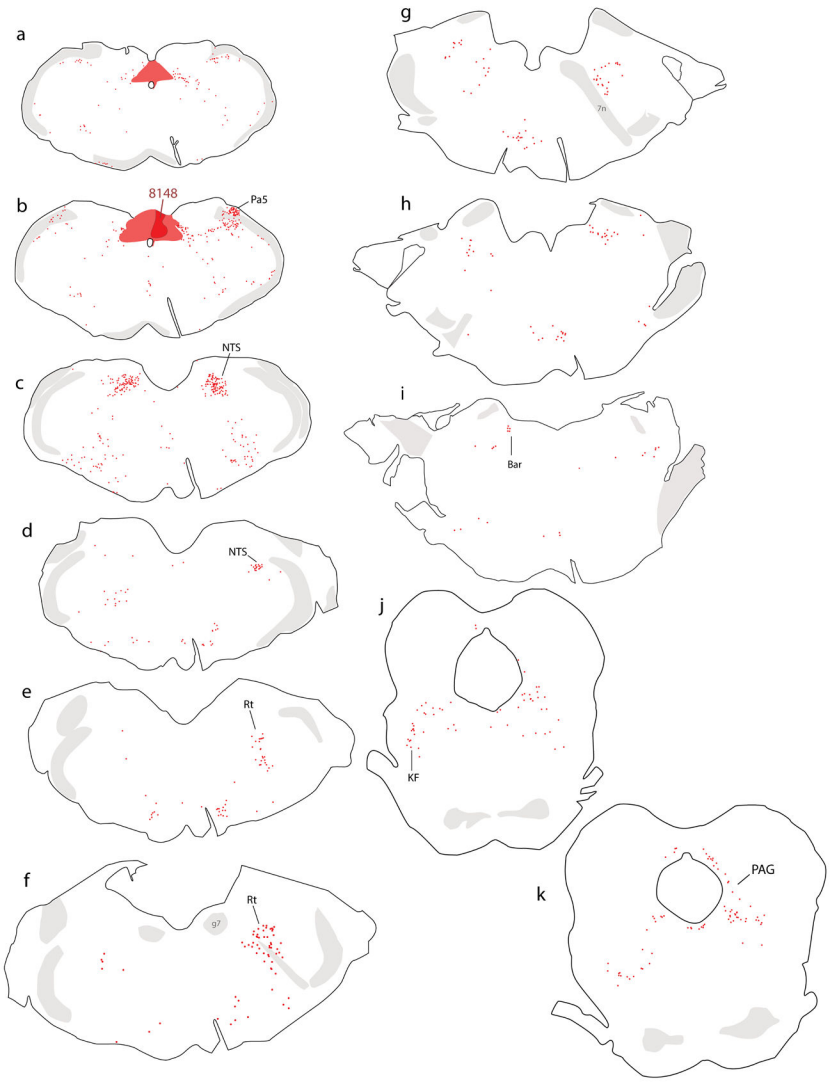

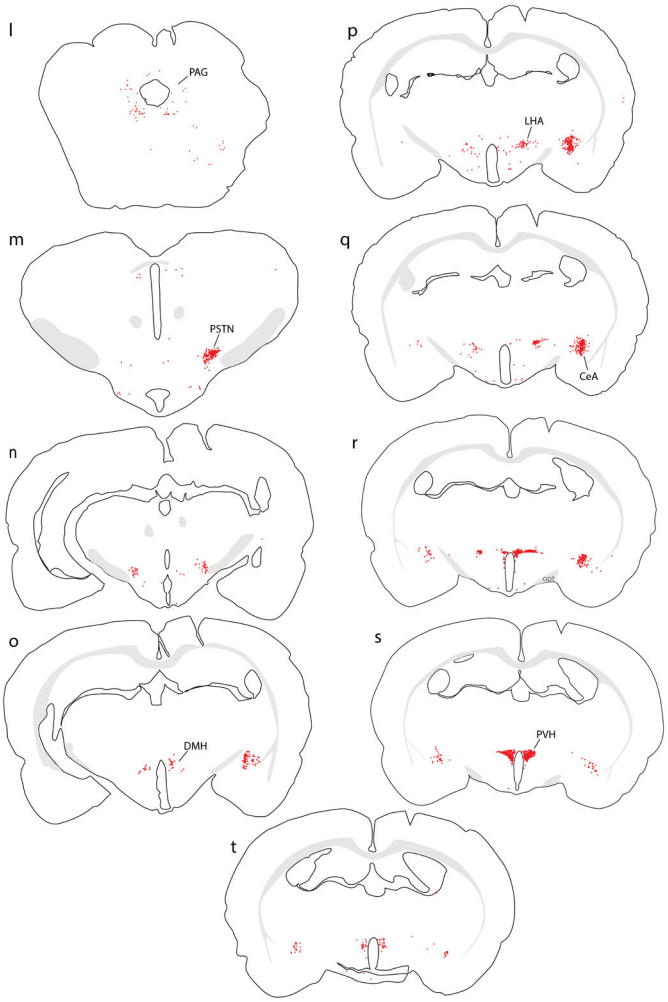

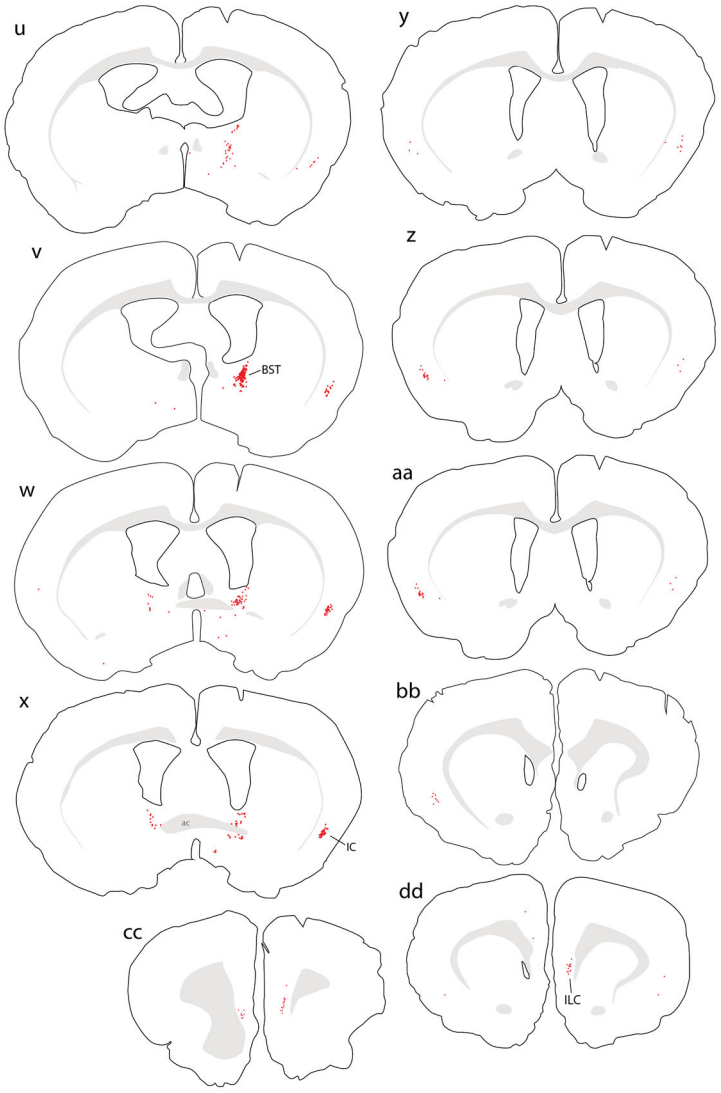

Figure 1.

Retrograde labeling throughout the brain after cholera toxin B subunit (CTb) injection into the NTS in rat. Abbreviations: 7n, cranial nerve 7 (facial nerve); ac, anterior commissure; Bar, Barrington's nucleus; BST, bed nucleus of the stria terminalis; CeA, central nucleus of the amygdala; DMH, dorsomedial nucleus of the hypothalamus; g7, genu of cranial nerve 7 (facial nerve); ILC, infralimbic cortex; KF, Kölliker-Fuse nucleus; LHA, lateral hypothalamic area; NTS, nucleus of the solitary tract; opt, optic tract; Pa5, paratrigeminal nucleus; PAG, periaqueductal gray matter; PSTN, parasubthalamic nucleus; PVH, paraventricular nucleus of the hypothalamus; Rt, brainstem reticular formation.

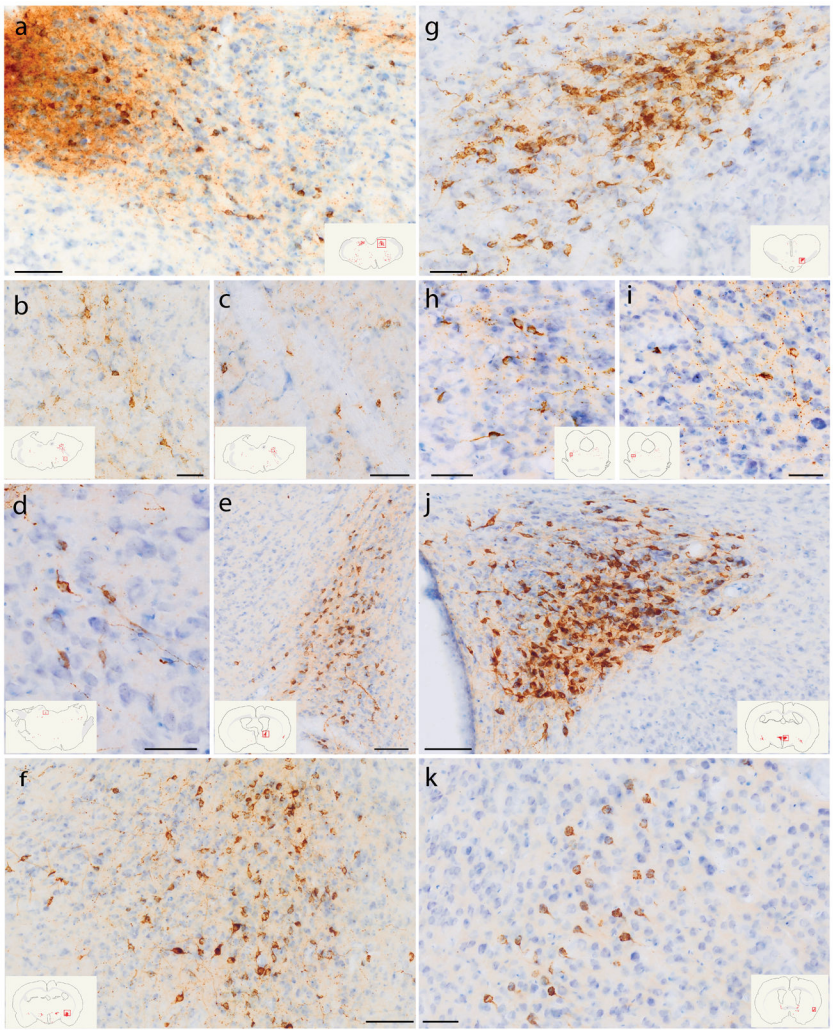

Figure 2.

CTb (brown) retrograde labeling in select regions of the rat brain, with light Nissl-counterstain (thionin, blue) for cytoarchitectural reference. Inset illustrations highlight the section (plotted in Figure 1) from which each photomicrograph was taken. (a) Rostral NTS; (b-c) hindbrain reticular nucleus along the intramedullary facial nerve fibers; (d) Bar; (e) dorsolateral BST; (f) Medial CeA; (g) PSTN; (h-i) KF region; (j) PVH; (k) mid-insular cortex. Scale bars are 50 μm (b-d, g-k) or 100 μm (a, e, f, j).

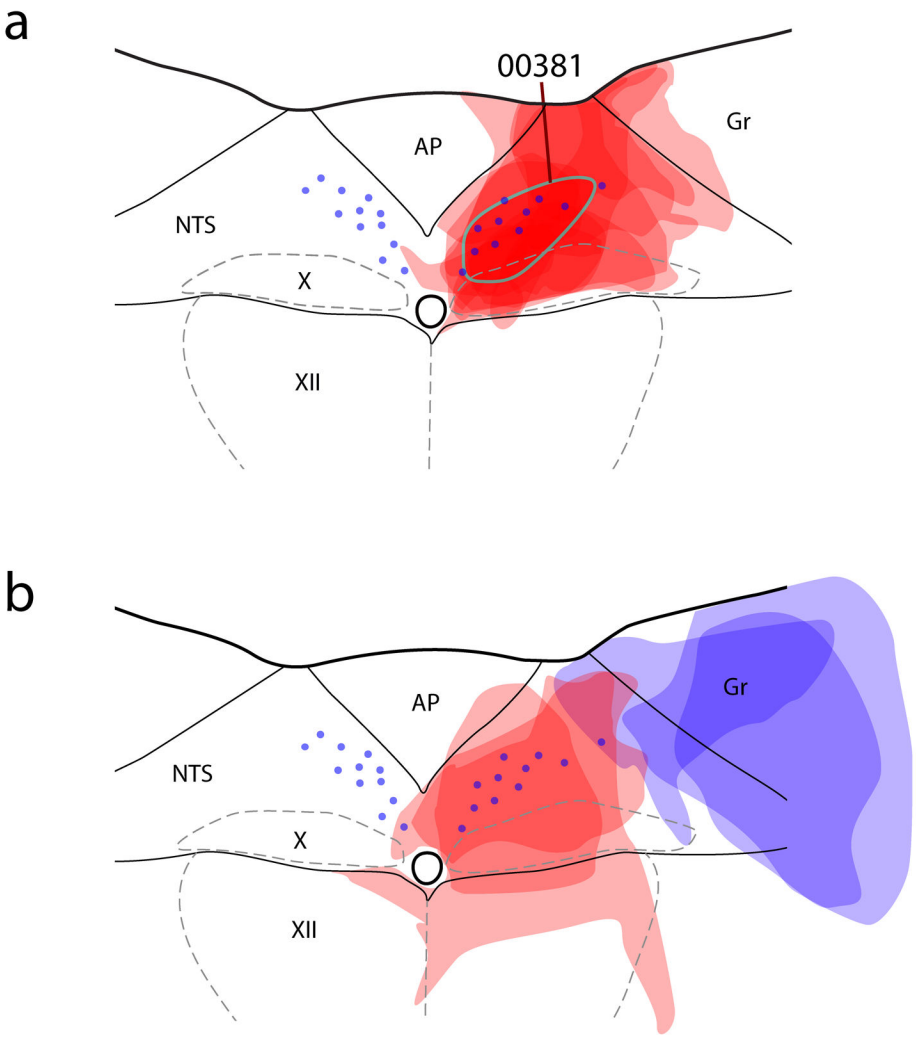

Figure 3.

Injection sites of all mice. (**a**) CTb injection sites are semi-transparent in red. Blue dots represent the distribution of NTS neurons containing immunoreactivity for 11-beta-hydroxysteroid dehydrogenase type 2 (HSD2), used to align the injection site drawing from each case. The CTb injection site from case #381, used for whole-brain illustration in the next figure, is highlighted with a blue-green outline. Double-retrograde injection cases are shown in (**b**), with CTb in red and fluorogold (Fg) injection sites in blue semi-transparency. Abbreviations: AP, area postrema; Gr, gracile nucleus; X, dorsal motor nucleus of the vagus nerve; XII, hypoglossal motor nucleus.

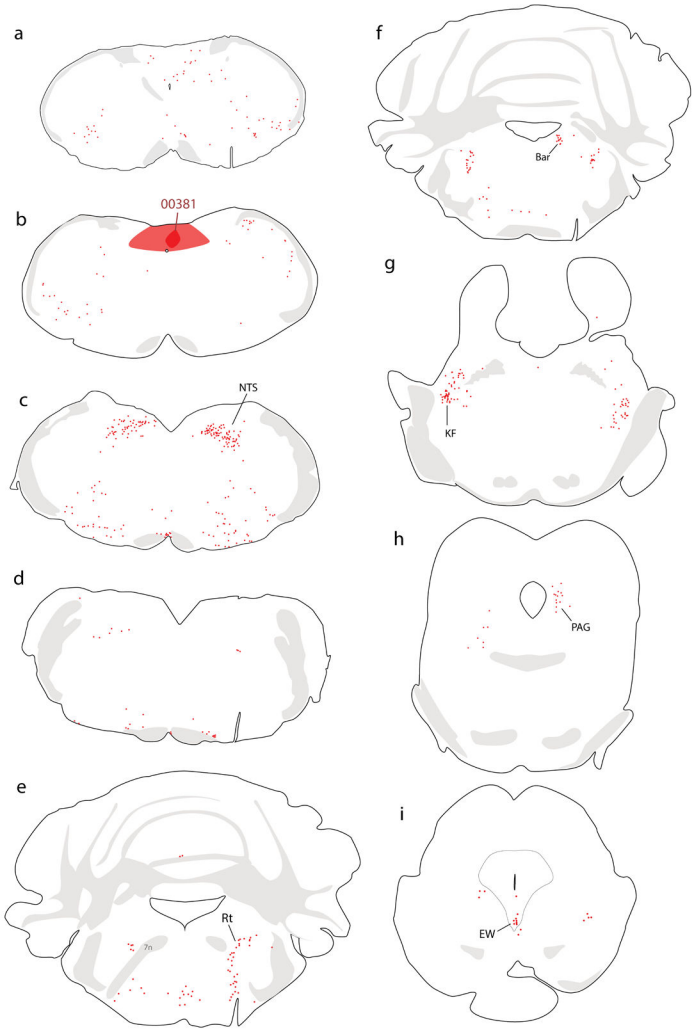

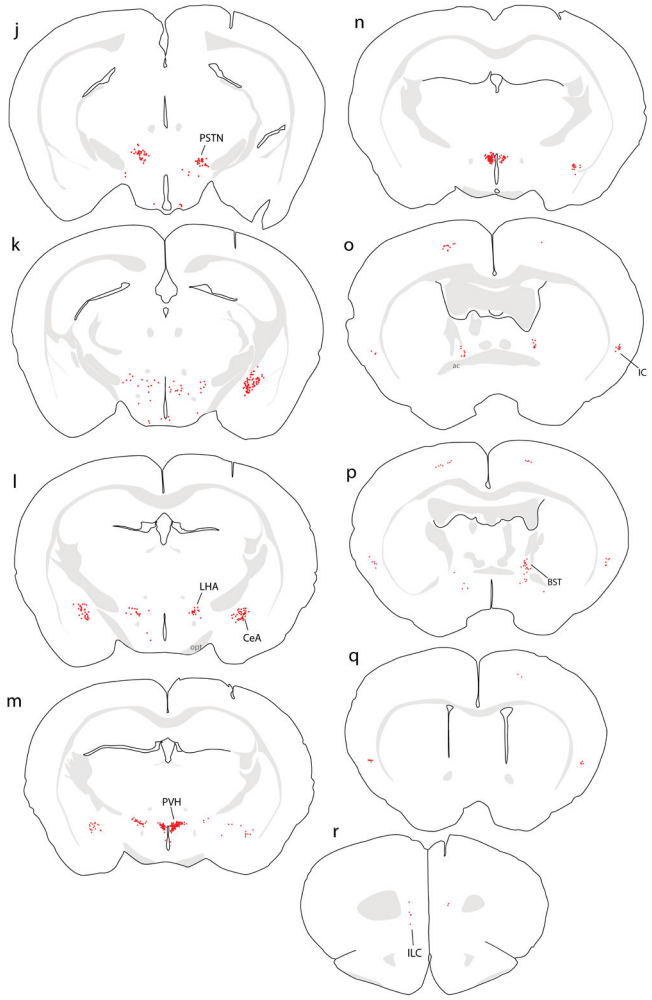

Figure 4.

Retrograde labeling throughout the brain after CTb injection into the NTS in mouse. Additional abbreviations: EW, Edinger-Westphal nucleus.

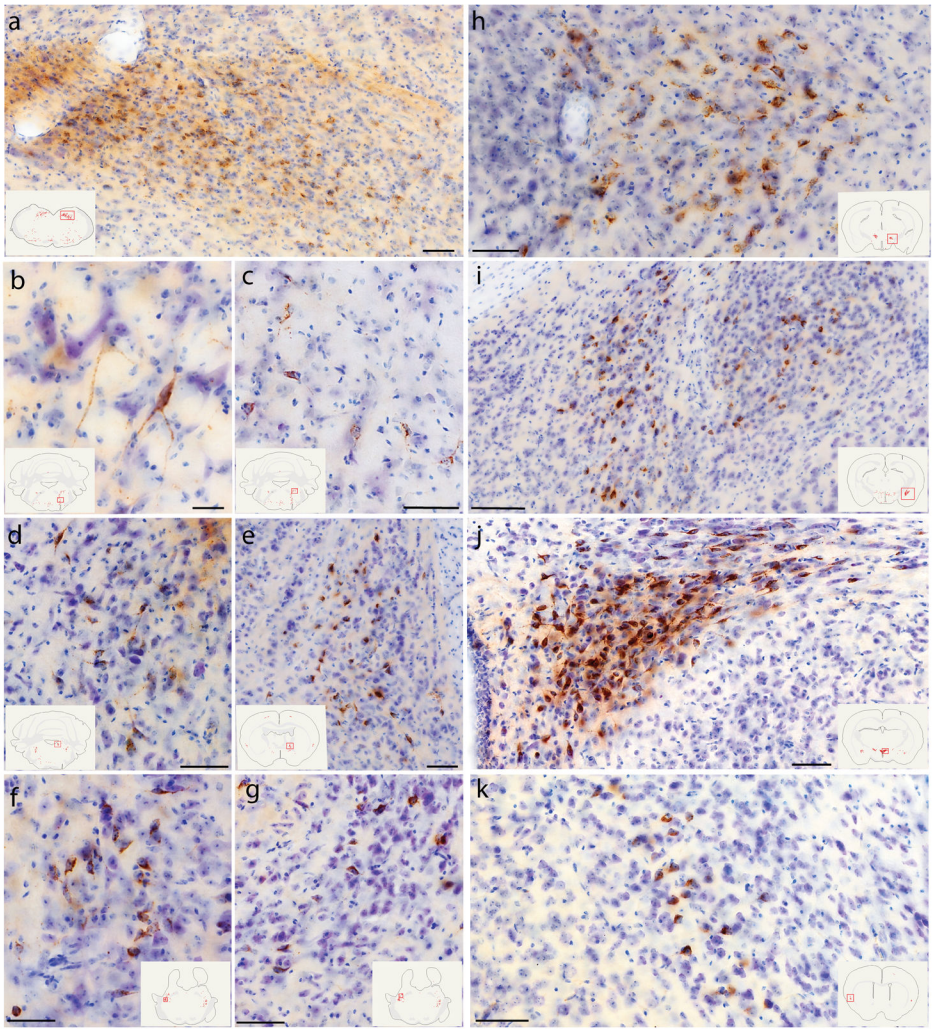

Figure 5.

CTb (brown) retrograde labeling in select regions of the mouse brain, with light Nissl-counterstain (thionin, blue) for cytoarchitectural reference. In each panel, the inset illustration highlights the region from which each photomicrograph was taken. (a) Rostral NTS; (b-c) hindbrain reticular nucleus; (d) Bar; (e) dorsolateral BST; (f-g) KF region; (h) PSTN; (i) CeA; (j) PVH; (k) mid-insular cortex. All scale bars are 50 μm.

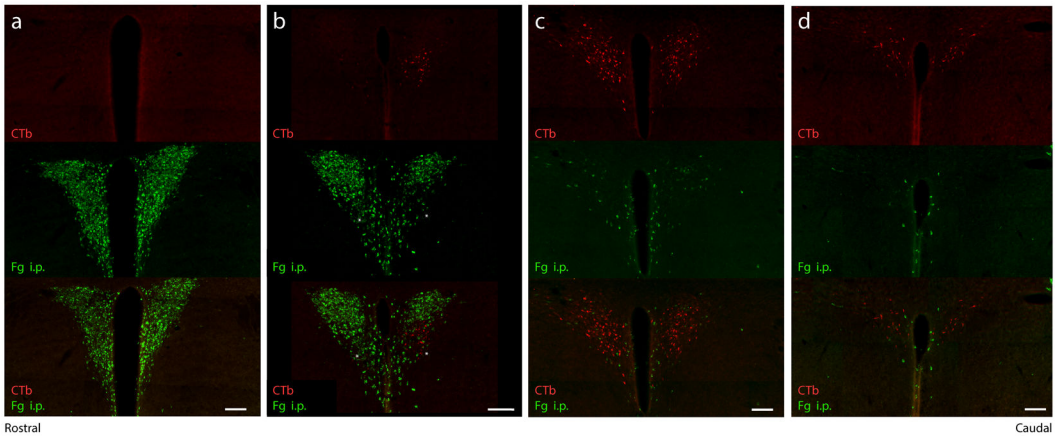

Figure 6.

Consecutive rostral-to-caudal levels of the PVH (A-D, 1-in-3 40 μm brain sections) showing Fg (green) uptake from systemic (intraperitoneal) injection and CTb retrograde labeling (red) after injection into the NTS. Magnocellular and parvocellular neuroendocrine neurons in the PVH (green) are entirely distinct from (and largely rostral to) PVH neurons that project axons to the NTS (red). Scale bars are 100 μm.

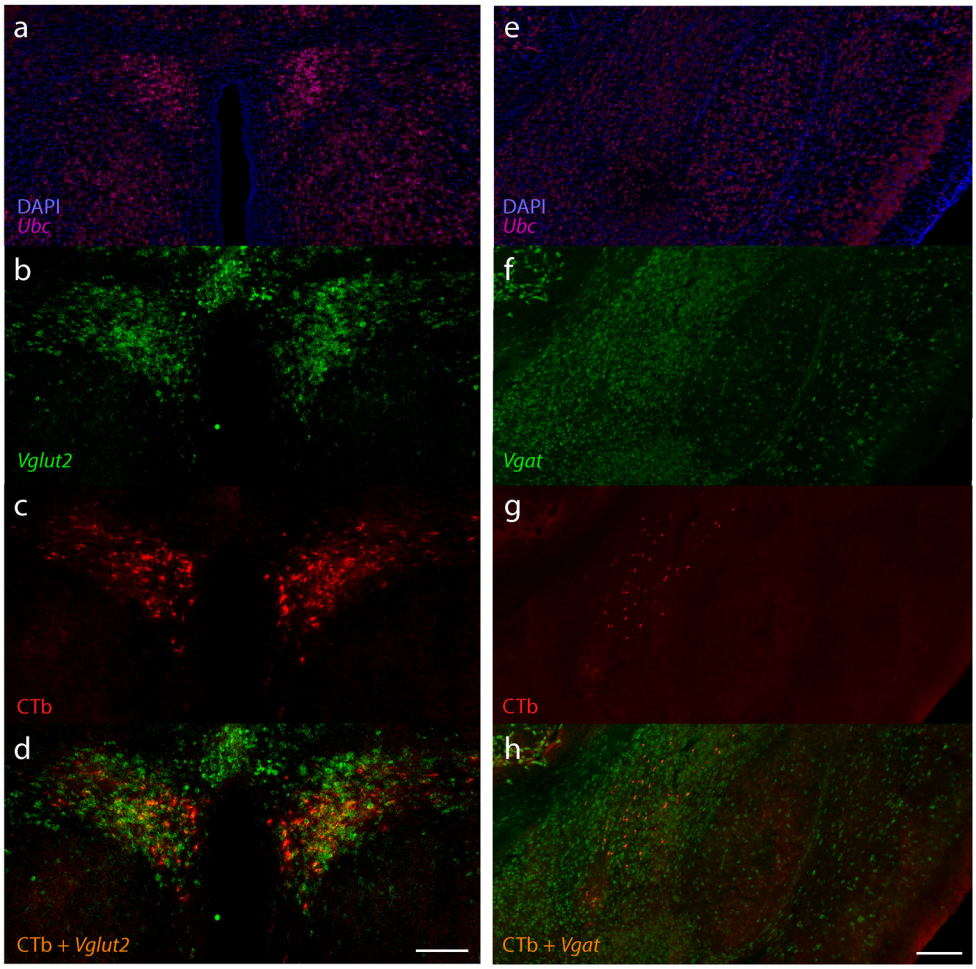

Figure 7.

(**a-d**) Expression of mRNA for the vesicular glutamate transporter 2 (Vglut2/*Slc17a6*, green) shows that CTb retrogradely labeled neurons in the PVH are glutamatergic. (**e-h**) Expression of mRNA for the vesicular GABA transporter (Vgat/*Slc32a1*, green) shows that CTb retrogradely labeled neurons in the CeA are GABAergic. In both cases, the ubiquitously expressed *Ubc* (green) and DAPI nuclear counterstain are shown for background comparison. Scale bars are 200 μm.

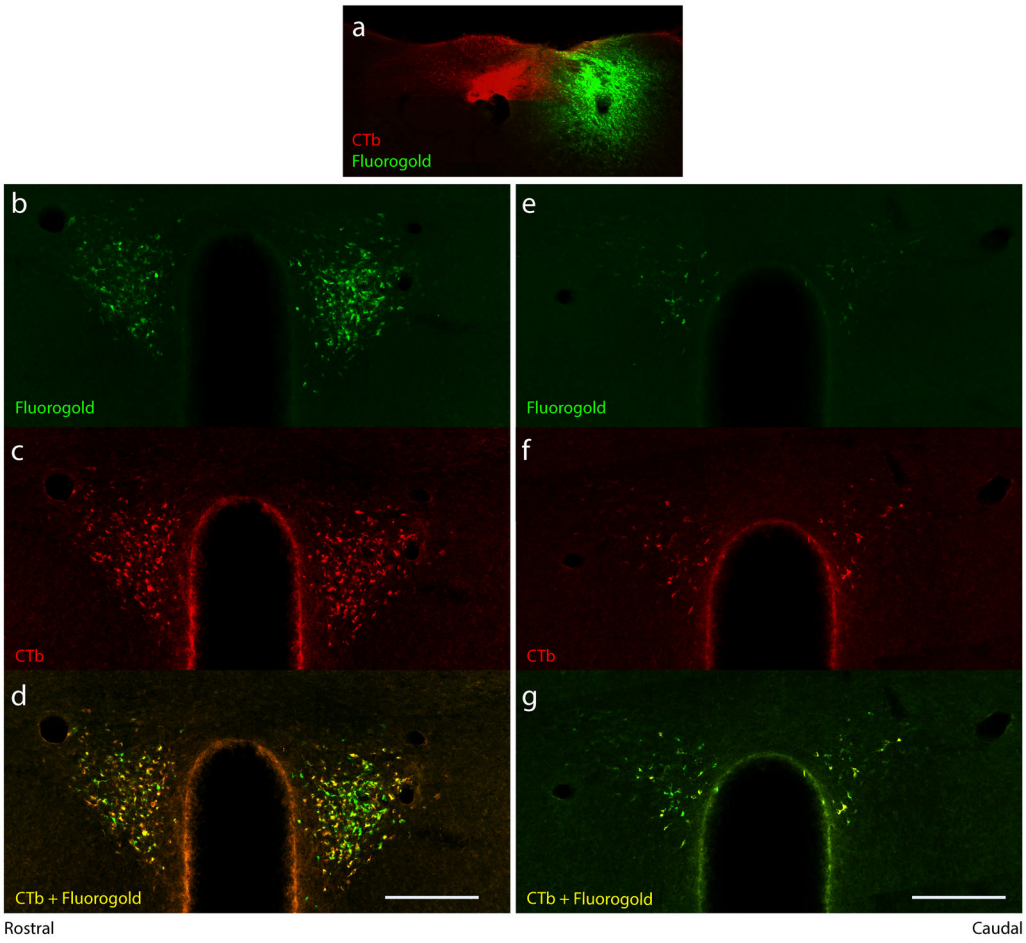

Figure 8.

Double-retrograde labeling from the medial and lateral NTS. (**a**) CTb injection into the medial NTS (red) with Fg injection targeting the lateral NTS (green) retrogradely labeled (**b-g**) overlapping and largely co-localized neurons in the PVH. Scale bars are 200 μm.

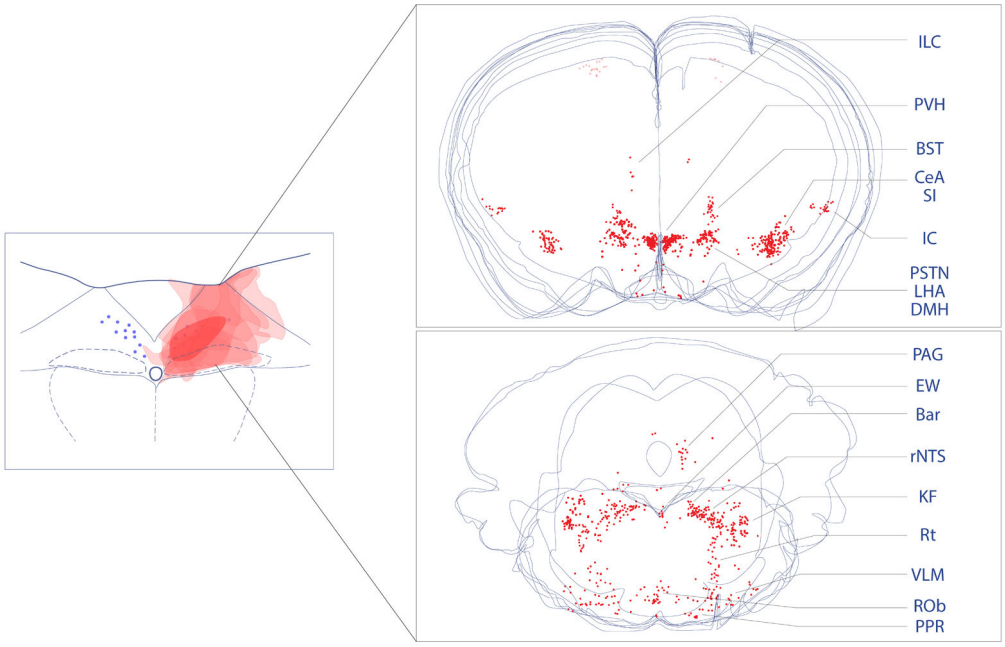

Figure 9.

Overall distribution of neurons that project axons to the NTS. To produce these summary images, we overlaid plots of CTb retrograde labeling (red, Figure 3) from the forebrain (top) and brainstem (bottom). CTb-labeled neurons in the motor cortex are faded because anterograde labeling studies from this one site show a lack of projections to the NTS (see text).

Table 1.

Antisera used in this study.

Antigen	Immunogen description	Source, Host Species, RRID	Concentration
11-beta-hydroxysteroid dehydrogenase type 2 (HSD2)	Raised against amino acids 261-405 of the C-terminus of human 11β-HSD2	Santa Cruz, rabbit polyclonal, cat. #sc_20176, lot #B0609, AB_2233199	1:700
Fluorogold	Fluorogold (*glutaraldehyde conjugate)*	Protos Biotech Corp, guinea pig polyclonal, cat. #NM-101. RRID: AB_2314409	1:500
Cholera Toxin B (CTb)	Purified choleragenoid, the B subunit of cholera toxin	List Biological, goat polyclonal, cat. #703, lot #7032A9, RRID: AB_10013220	1:10,000

Table 2.

Fluorescence *in situ* hybridization probes used in this study:

Probe	Common Name	Channel	ACD Catalog #	Lot #
Mm-Slc17a6	Vesicular glutamate receptor 2	C1	319171	17251A
Mm-Slc32a1-C3	Vesicular GABA transporter	C3	319191-C3	18038A
Mm-Ubc	Ubiquitin C	C1	310771	18010A
Mm-Ubc-C2	Ubiquitin C	C2	310771-C2	18095B

Table 3.

CTb-labeled neuron counts in select brain regions.

Case	rNTS	Rt	Bar	PSTN	CeA	PVH	BST	IC
00381	80	47	15	55	91	80	40	8
00385	76	30	7	48	92	83	14	15
00481	61	15	8	32	62	45	12	5
00483	62	23	11	15	44	60	18	7
00522	24	5	4	25	25	34	6	5
Mean	**60.6**	**24.0**	**9.0**	**35.0**	**62.8**	**60.4**	**18.0**	**8.0**
Std.	22.1	15.9	4.2	16.4	29.3	21.4	13.0	4.1